[American Journal of Science, Vol. 301, March, 2001, P. 261–285]

CHEMOSTRATIGRAPHY OF THE PALEOPROTEROZOIC DUITSCHLAND FORMATION, SOUTH AFRICA: IMPLICATIONS FOR COUPLED CLIMATE CHANGE AND CARBON CYCLING

ANDREY BEKKER*, ALAN J. KAUFMAN**, JUHA A. KARHU***, NICOLAS J. BEUKES****, QUINTEN D. SWART****, LOUIS L. COETZEE****, and KENNETH A. ERIKSSON*

ABSTRACT. The Paleoproterozoic Duitschland Formation lies stratigraphically beneath the Timeball Hill Formation, which contains the only unequivocal glacial unit of this era in the Transvaal Basin, South Africa. Lithologic evidence in Paleoproterozoic successions of North America, however, indicates the existence of three discrete and potentially global ice ages within this 300 my interval. Carbonates of the Duitschland Formation are significantly enriched in ^{13}C up to +10.1 permil in the upper part of the succession above a notable sequence boundary. In contrast, the lower part of this unit contains carbonates with consistently negative $\delta^{13}C$ values. Trace and major element compositions of these carbonates as well as carbon-isotopic compositions of coexisting organic matter support a primary origin for the markedly positive carbon isotope anomaly. The stratigraphic constraints indicate that ^{13}C-enriched carbonates were deposited prior to Paleoproterozoic glaciation in southern Africa, similar to carbonates stratigraphically beneath Neoproterozoic glacial diamictites worldwide. Also mirroring the Neoproterozoic record are strongly negative $\delta^{13}C$ values in cap carbonates atop glacial diamictites in Paleoproterozoic strata of Wyoming and Ontario. The litho- and chemostratigraphic constraints indicate that the interval of negative carbon isotope values in well-preserved carbonates of the lower Duitschland Formation may reflect a second Paleoproterozoic ice age in the Transvaal succession. This interpretation is further supported by recently discovered bullet-shaped clasts with striations in diamictite from the basal part of the succession. Thus, the emerging temporal pattern of carbon isotope variations and glaciation in the Paleoproterozoic has a close analogue to Neoproterozoic events, suggesting a coupling of climatic and biogeochemical changes at both ends of the eon.

INTRODUCTION

The Paleoproterozoic Era (1.6-2.5 Ga) is a distinct interval in Earth history characterized by inter-related tectonic, evolutionary, climatic, and biogeochemical events resulting in broad changes of Earth's surface environments. The detailed relationship between key transitions is poorly understood, however, due to uncertainties in correlation and the age of sedimentary successions where critical events are preserved, as well as stratigraphic omissions and post-depositional insults that obscure the true nature of temporal trends. For example, in North America, three discrete levels of Paleoproterozoic glacial diamictites are recognized in the Huronian and Snowy Pass supergroups of Ontario and Wyoming (Young, 1973, 1988; Ojakangas, 1985), respectively; on other continents only a single unequivocal diamictite of glacial origin has thus far been recognized (Ojakangas, 1985). In North America, these ice ages are radiometrically constrained to have occurred over a 230 my interval between 2.22 and 2.45 Ga (fig. 1; Krogh, Davis, and Corfu, 1984; Corfu and Andrews, 1986).

*Department of Geological Sciences, Virginia Polytechnic Institute and State University, Blacksburg, Virginia 24061.

**Department of Geology, University of Maryland at College Park, College Park, Maryland 20742.

***Geological Survey of Finland, FIN-02150 Espoo, Finland, and Department of Geology, University of Helsinki, FIN-00014, Finland.

****Department of Geology, Rand Afrikaans University, Auckland Park 2006, Johannesburg, South Africa.

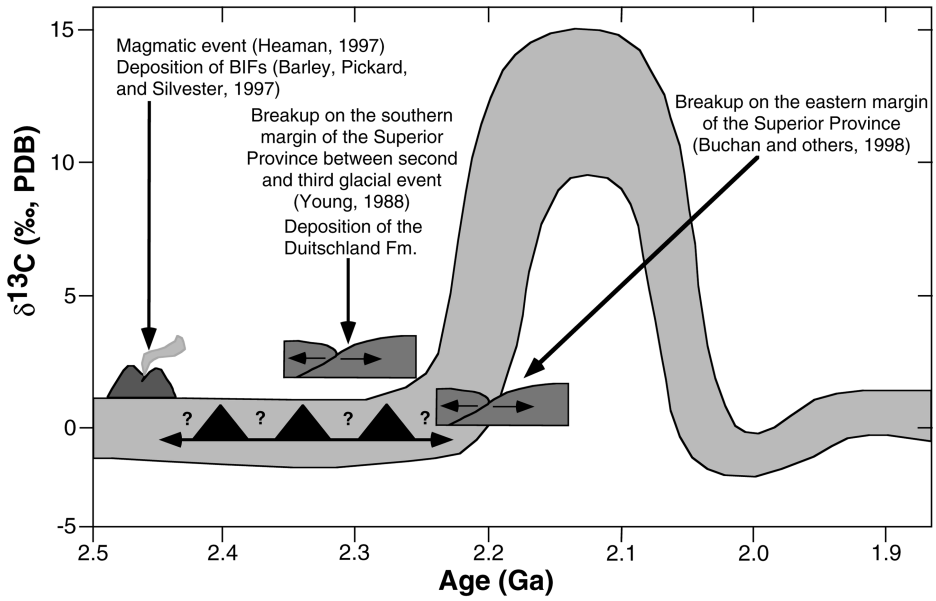

Fig. 1. Schematic representation of Paleoproterozoic $\delta^{13}C$ variations presented by Karhu and Holland (1996) and timing of key geological events through this interval. Black triangles and question marks between them represent three glacial events of the Paleoproterozoic in North America and their age uncertainty.

Karhu and Holland (1996) suggest that following the last of the Paleoproterozoic ice ages is a positive carbon isotope excursion whose extreme magnitude ($> +12$ permil; fig. 1) finds a match only in a narrow interval of Neoproterozoic time (0.545-1.0 Ga; Iyer and others, 1995; Misi and Veizer, 1998). This carbon isotope anomaly is best documented in 2.1 to 2.2 Ga old sedimentary sequences from Baltica (Baker and Fallick, 1989; Karhu, 1993; Melezhik and others, 1996) where only one stratigraphic level of glacial diamictite is recognized; notably, it lies below the biogeochemical anomaly.

Both ends of the Proterozoic Eon are characterized by (1) protracted intervals of tectonic assembly (resulting in the formation of the supercontinents known as Kenoraland and Rodinia) and breakup; (2) oscillations between greenhouse and icehouse conditions; and (3) significant changes in the composition of the atmosphere and ocean, and, in particular, strong carbon isotope excursions. However, in contrast with the known Paleoproterozoic record of isotopes and ice ages (with the biogeochemical anomaly following the last known glaciation), the high resolution Neoproterozoic record reveals that strongly positive-to-negative $\delta^{13}C$ of seawater proxies bracket at least two (Kennedy and others, 1998) and perhaps as many as four or more (Kaufman, Knoll, and Narbonne, 1997; Corsetti and Kaufman, 1999) discrete glaciations. In particular, strongly positive $\delta^{13}C$ in carbonates characterize pre-glacial successions while negative $\delta^{13}C$ anomalies occur in all "cap carbonates" atop Neoproterozoic diamictites. These enigmatic biogeochemical and climatic events are viewed as a response to extreme modulations in atmospheric CO_2 concentrations (Kaufman, Knoll, and Narbonne, 1997; Hoffman, Kaufman, and Halverson, 1998; Hoffman and others, 1998) at a time when 6.5 percent less radiant energy was reaching the planet's surface relative to today (Kasting, 1987). Lowering of CO_2 below threshold concentrations plausibly plunged the planet into a runaway glaciation that resulted in high albedo "Snowball Earth" conditions, where the oceans were blanketed in a thick cover

of sea ice for millions of years (Kirschvink, 1992; Hoffman and others, 1998). This hypothesis is consistent with paleomagnetic data for equatorial glaciation at sealevel in the Neoproterozoic of Australia (Schmidt, Williams, and Embleton, 1991; Sohl, Christie-Blick, and Kent, 1999) and arctic Canada (Park and others, 1997).

In the early Paleoproterozoic, when the solar output is estimated to be only 82 percent of the modern (Kasting, 1987), paleomagnetic studies in South Africa and Canada also point to the probability of low latitude glaciation (Evans, Beukes, and Kirschvink, 1997; Williams and Schmidt, 1997; Buchan and others, 1998; Schmidt and Williams, 1999; see also Mertanen and others, 1999 for a potential low latitude position of Baltica). If Snowball Earth-like conditions punctuated surface environments in both intervals, why is the temporal relationship between ice ages and extreme carbon isotope excursions different at the beginning and end of the Proterozoic Eon?

To investigate this question, in particular whether extreme ^{13}C enrichments characterize carbonates beneath glacial strata of Paleoproterozoic age, we chose to study well-preserved carbonates of the Duitschland Formation in South Africa. This succession lies stratigraphically below the glaciogenic Timeball Hill Formation (Visser, 1971-1972). Highly positive carbon isotope values have been reported previously in carbonates altered by contact metamorphism from the upper Duitschland Formation (Buick and others, 1998). Insofar as samples of this study were collected at high resolution within a sequence stratigraphic framework and diagenetic tests were conducted to evaluate the degree of sample alteration, this research differs considerably from all previous chemostratigraphic studies of Paleoproterozoic strata. In addition, carbon isotope compositions of coexisting organic matter were determined to further evaluate the primary nature of carbon isotope variations.

REGIONAL GEOLOGY AND STRATIGRAPHY

Paleoproterozoic successions in South Africa are preserved in the Transvaal and Griqualand West basins. The Vryburg Rise (fig. 2; Button, 1986) presently separates these once contiguous deposits. Lithostratigraphic correlation between the structural sub-basins is supported by available chronostratigraphic data and based on several marker-beds including: (1) thick stromatolitic carbonate platform facies (Campbellrand and Malmani subgroups); (2) banded iron-formation (Griquatown, Kuruman, and Penge IFs); (3) glacial diamictite and associated units (Makganyene Diamictite and upper part of the Timeball Hill Formation); and (4) thick volcanics of intermediate composition (Ongeluk andesite and Hekpoort Formation). A glaciomarine environment of deposition was inferred for the upper part of the Timeball Hill Formation (Visser, 1971-1972) and the equivalent Makganyene Diamictite (Visser, 1981) based on the presence of striated, pock-marked, and faceted pebbles, as well as laminated shales. Based on paleomagnetic data from the Ongeluk andesite, a unit overlying the glacial diamictite, a low latitude position for the Kaapvaal Craton during this ice age was inferred (Evans, Beukes, and Kirschvink, 1997).

The Duitschland Formation sits at the base of the Pretoria Group in the Transvaal Basin (fig. 3) and is a time equivalent of the Rooihoogte Formation (Swart, ms). A maximum age constraint for the Duitschland Formation is based on 2480 ± 6 Ma U-Pb SHRIMP age for the underlying Penge Iron-Formation (A.F. Trendall, unpublished data in Nelson, Trendall, and Altermann, 1999). A tentative minimum age limit for the Chuniespoort Group including the Duitschland Formation is based on Pb-Pb whole rock dating of the Ongeluk andesites in the lithostratigraphically equivalent Ghaap Group of the Griqualand West Basin at 2222 ± 13 Ma (Cornell and others, 1996). This age, however, was not confirmed by U-Pb SHRIMP zircon study and is likely related to a heterogeneous initial Pb isotopic composition (Bau and others, 1999). In addition, the Moodraai Dolomite, stratigraphically above the Ongeluk andesite in the Griqualand West Basin, has a Pb-Pb isotopic carbonate age of 2394 ± 26 Ma (Bau and others,

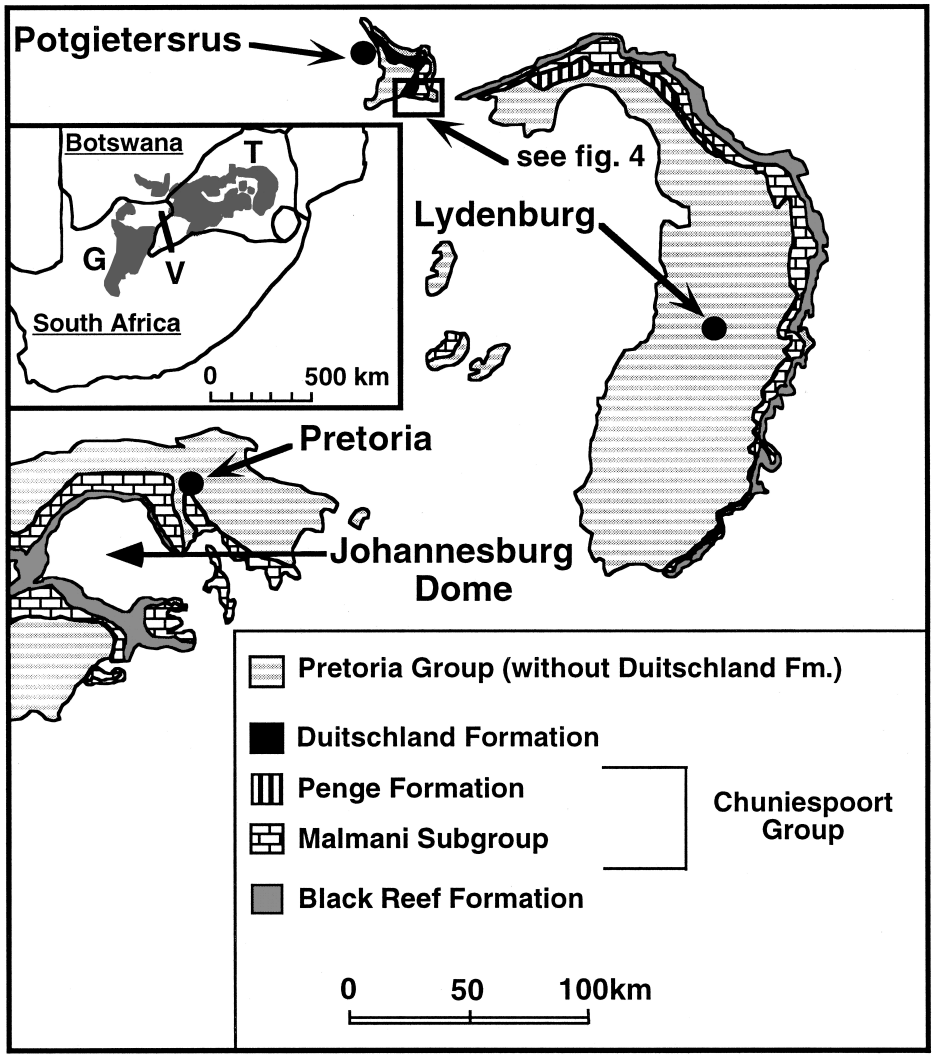

Fig. 2. Simplified geological map showing Potgietersus area where sections of the Duitschland Formation were studied. Inset shows the Griqualand West (G) and Transvaal (T) basins and Vryburg (V) rise. See Fig. 4 for the detailed map of the Potgietersus area.

1999). When combined, these ages with their uncertainties constrain the Timeball Hill glaciation and deposition of the Duitschland Formation between 2486 and 2368 Ma.

The Duitschland Formation is exposed in two areas near Potgietersrus in the northern part of the Olifants River Valley (figs. 2 and 4; Martini, 1979). In these areas an unconformity at the base of the Duitschland Formation separates this unit from ~50 m thick laminated, ferruginous dolomite rhythmites of the underlying Tongwane Formation (fig. 3). These dolomites are considered to be conformable with the underlying Penge Iron Formation (Martini, 1979). In the eastern Transvaal Basin, erosional unconformity separates the Duitschland Formation from the overlying Timeball Hill Formation. Regionally, however, a paraconformable contact between the Duitschland and Timeball Hill formations has been observed (Swart, ms). Accordingly, the Duitschland Formation is included in the basal part of the Pretoria Group.

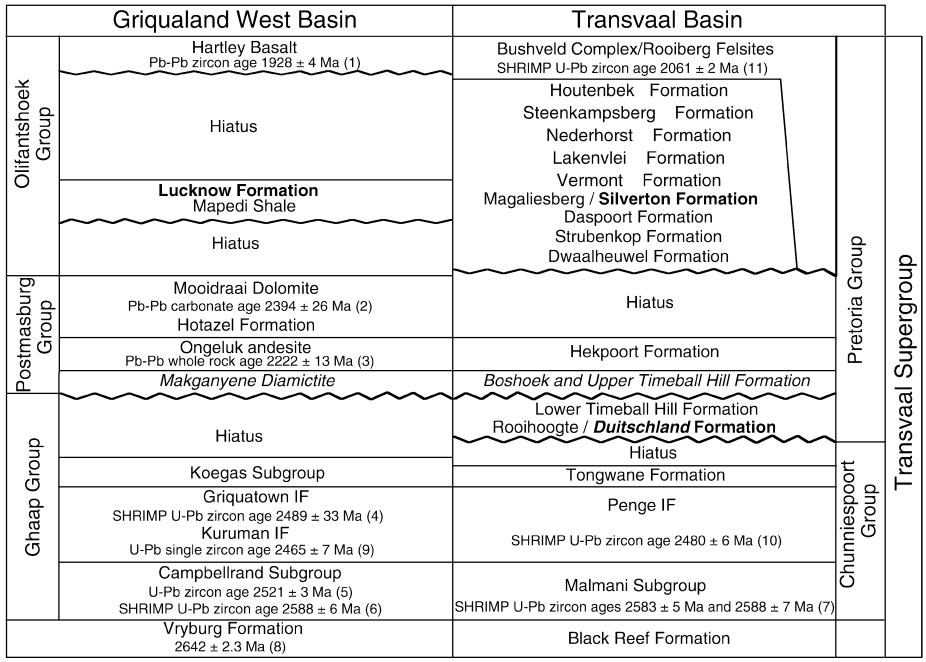

Fig. 3. Correlation chart for the lower part of the Transvaal Supergroup in the Griqualand West and Transvaal structural basins, South Africa (after Swart, ms and Dorland, ms). Sources of ages: 1 – Cornell, Armstrong, and Walraven, 1998; 2 –Bau and others, 1999; 3 – Cornell, Schütte, and Englinton, 1996; 4 – Trendall unpubl. data in Nelson, Trendall, and Altermann, 1999; 5 – Sumner and Bowring, 1996; 6 – Altermann and Nelson, 1998; 7 – Martin and others, 1998; 8 – Walraven and others, in press, in Nelson, Trendall, and Altermann, 1999; 9 – Armstrong, pers. com., 1996, in Martin and others, 1998; 10 – Trendall unpubl. data in Nelson, Trendall, and Altermann, 1999; 11 – Walraven, Armstrong, and Kruger, 1990; McNaughton and Pollard, 1993; Walraven, 1997. Units in bold type contain ^{13}C-enriched carbonates and units in italics contain diamictites.

Martini (1979) recognized several stratigraphic levels of diamictite in the Duitschland Formation (fig. 5), but evidence linking these to glacial activity was not presented. Recently, the basal diamictite of the Duitschland Formation has been interpreted as glacial in origin based on its (1) basin wide distribution, (2) heterogeneous composition of clast types (including basement rocks and BIF), and (3) presence of clear striations on *in situ* bullet shaped quartzite pebbles and cobbles (fig. 6A; Coetzee, ms; Beukes and others, 2001).

The Duitschland Formation was studied in the type area 20-km southeast of Potgietersrus on Duitschland Farm as well as exposures on DeHoop and Langbaken farms (fig. 4). This succession has a thickness of about 1000 m and is clearly divided into two parts by a notable sequence boundary marked by conglomerate at the base of the quartzite unit (fig. 5; Swart, ms). The lower half begins with chert edge-wise conglomerate and the glacial diamictite overlain by thick, finely-laminated carbonaceous shale, which is in turn overlain by interbedded layers of limestone, marl, and breccia. Carbonate layers are thin and composed of gray, finely laminated limestone rhythmites, likely deposited in deep water below storm wave base. Chert and limestone breccias in the lower part of the succession are interpreted as a gravity flow slope deposit (Swart, ms). Quartzite and dolomite dominate near the top of this upward-shallowing succession.

The upper half of the formation starts with fine- to coarse-grained quartzite and conglomerates that fine upward into shale. The shale then forms the base of two

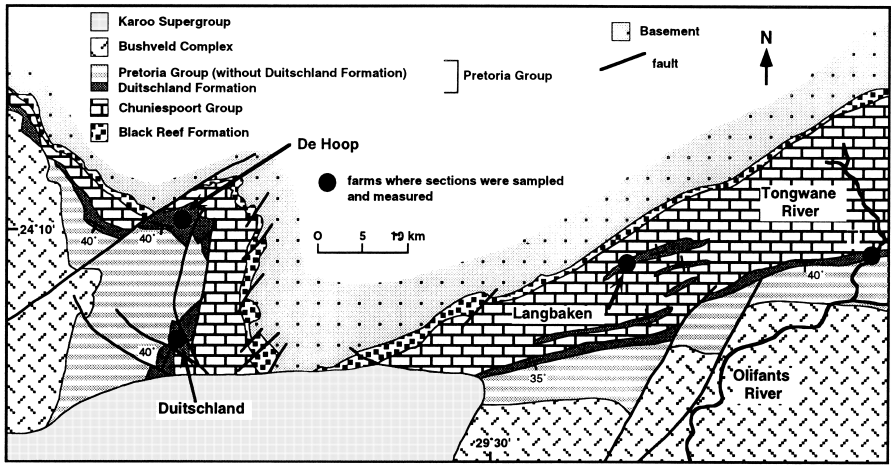

Fig. 4. Detailed map of the Potgietersus area with locations of sampled sections of the Duitschland and Tongwane formations. T is location where Tongwane Formation was sampled.

upward-shallowing shale-carbonate cycles (fig. 5). Above the basal conglomeritic quartzite, the cycles consist of shale with minor quartzite, carbonate, and breccia. An up section decrease in the abundance of shale and the presence of ripple marks in fine-grained quartzite at the top of the first cycle suggest that deposition occurred in shallow water environments. The first thick carbonate is limestone composed of isopachous sheet cements (= laminated tufa) likely formed as synsedimentary cements on the seafloor (fig. 6B; Hoffman, 1975; Grotzinger, 1994; Kah and Knoll, 1996). The overlying shale and carbonate are intruded by two sills emanating from the nearby Bushveld Complex, which produced contact metamorphism of some carbonates in this part of the section (fig. 5; Buick and others, 1998). The carbonate bed above the first sill is a light-colored ivory and pink shallow-water limestone with nodules and large stromatolitic domes (Martini, 1979). The overlying dolomite layer in the same cycle is also stromatolitic near its base but contains oolites and fan-shaped chert nodules as well as ripple-marked red to yellow dolomite with flaser muddy laminations above.

A chert breccia with a muddy matrix at the top of the second upward shallowing cycle is interpreted as a mudflow deposit (Swart, ms). The uppermost upward-shallowing cycle includes three ivory-colored dolomite beds with domal stromatolites, as well as silicified giant ooids (up to 0.5 cm) and grapestones (fig. 6C). These large, spherical coated grains must have required considerable wave energy to form (Sumner and Grotzinger, 1993) and are therefore most-likely marine in origin. These coated grains differ from vadose zone pisolites insofar as they are perfectly round, well sorted, and locally abundant. The final cycle terminates with a stromatolitic, cherty dolomite and a karstic chert breccia at the very top (Swart, ms), overlain sharply by black carbonaceous shale of the Timeball Hill Formation (fig. 5).

Although the Duitschland Formation is only locally preserved in the northeastern part of the Transvaal Basin, we infer a marine depositional environment for this succession. This view is consistent with sedimentologic evidence in the paraconformably overlying Timeball Hill Formation, which includes deep-water contourites near the base and tidally influenced deltaic deposits (Eriksson and Reczko, 1998). In addition, the giant spherical ooids and grapestones of the upper Duitschland strongly resemble those found in dominantly marine Neoproterozoic successions in Svalbard (Swett and Knoll, 1989), Namibia (Hegenberger, 1993), and the Great Basin, United

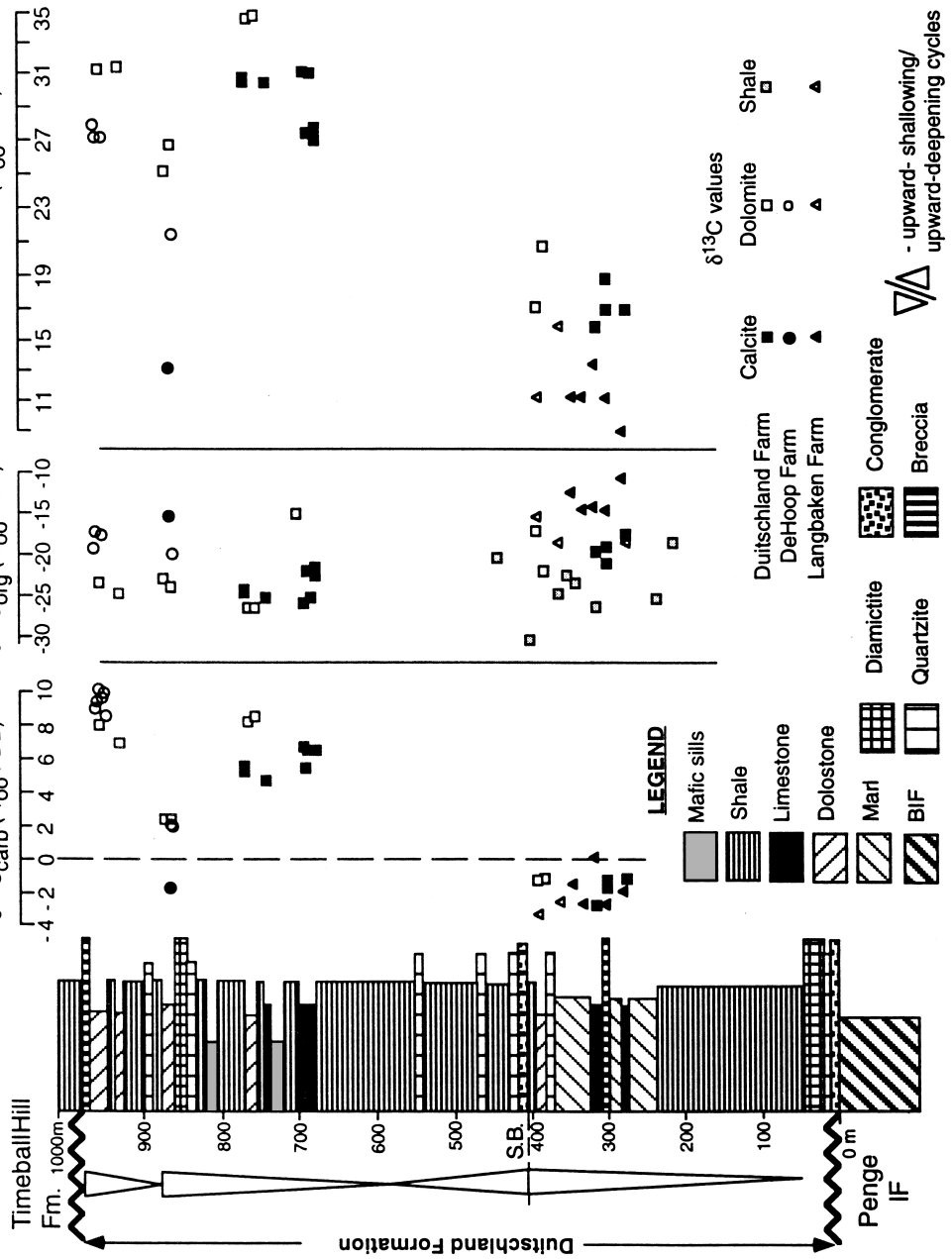

Fig. 5. Generalized stratigraphic column of the Duitschland Formation with measured variations in $\delta^{13}C_{carb}$, $\delta^{13}C_{org}$ and $\Delta\delta$ from Duitschland, DeHoop, and Langbaken farms.

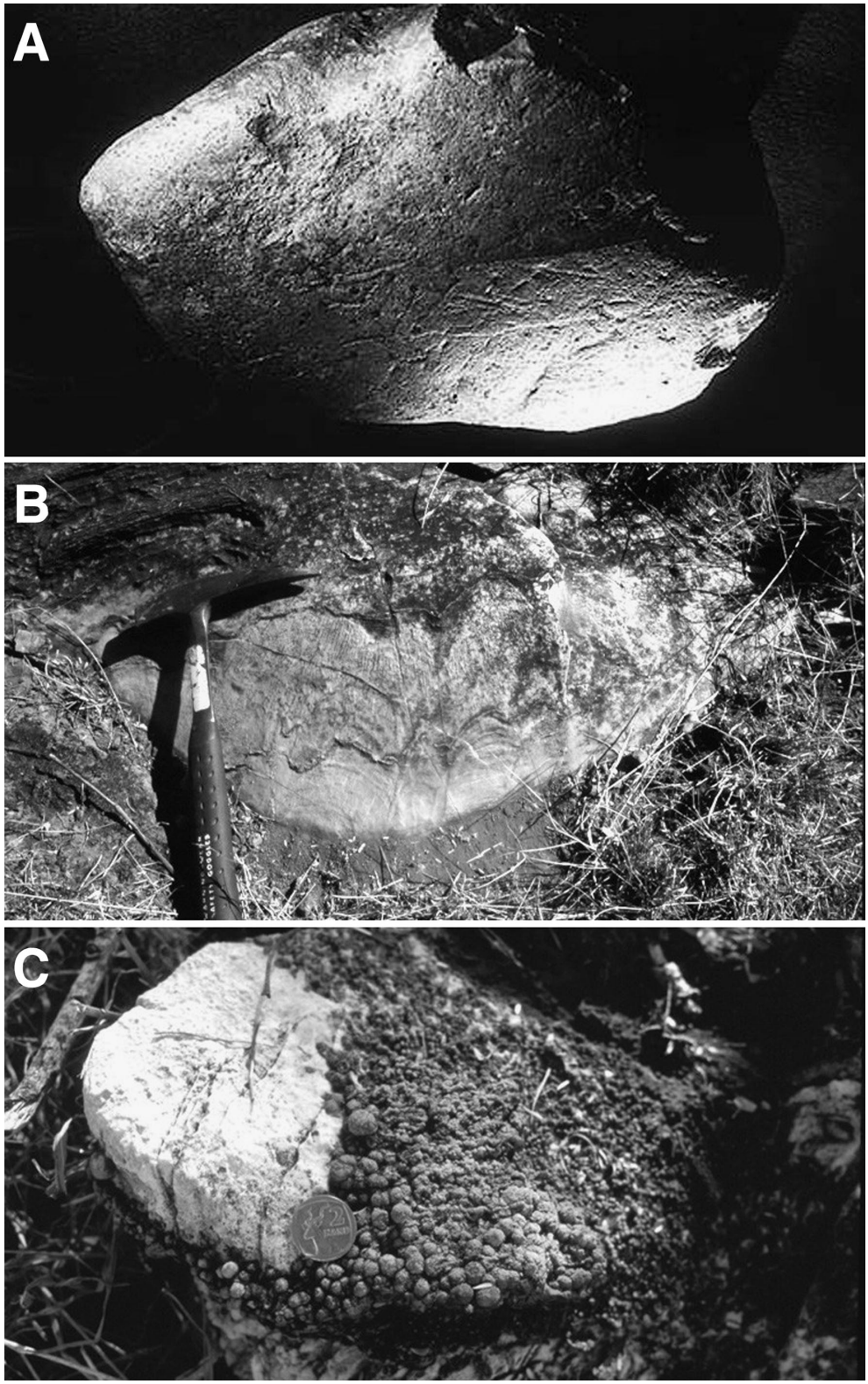

Fig. 6. (A) striated quartzite cobble plucked from the lower Duitschland puddingstone diamictite; (B) isopachous sheet cements from the upper Duitschland Formation; (C) giant ooids and grapestones from the upper part of the Duitschland Formation.

States of America (Tucker, 1986). Finally, the high Sr concentration in some samples and low $^{87}Sr/^{86}Sr$ of the isopachous cements (see below) strongly suggest an open marine setting and original aragonitic precursor (Veizer, 1983).

METHODS

Whole-rock powders were prepared from samples collected from the measured sections. Major and trace element concentrations were determined through the dissolution of ~10 mg of carbonate in 5 ml of 0.5 M acetic acid and subsequent analysis by ICP-AES at the Geological Survey of Finland (table 1). Uncertainties in the analytical data based on the measurement of multiple standard materials by this method are 5 percent for major elements and better than 10 percent for trace elements.

Carbon dioxide was extracted at the Geological Survey of Finland from whole-rock powders by closed tube reaction with anhydrous phosphoric acid ($\rho >$ 1.89 g/cc; 16+ hours) at a temperature of 25°C for limestone and for 1 hr at 100°C for dolomite; resulting CO_2 was isolated by cryogenic distillation for mass spectrometric analysis on a Finnigan MAT 251. The fractionation factors used for mineral correction of oxygen isotopes in calcite prepared at 25°C and dolomite at 100°C were 1.01025 and 1.00913, respectively. A second generation of carbonate samples (KB99 series) was micro-drilled, and the powders reacted with anhydrous phosphoric acid at 90°C in a Micromass Multiprep carbonate device; the resulting carbon dioxide was then measured with a Micromass Optima mass spectrometer at Rutgers University. The fractionation factors used for mineral correction of oxygen isotopes in calcite and dolomite prepared at 90°C were 1.00798 and 1.00895, respectively. For both techniques, the external precision based on multiple standard measurements of NBS-19 was better than 0.1 permil versus V-PDB for both carbon and oxygen.

Total organic carbon (TOC) was isolated from the carbonate samples by repeated acidification and centrifugation with concentrated HCl followed by washing until the sample reached neutral pH (Kaufman and Knoll, 1995). Dried samples in Vycor tubes were then mixed with CuO as an oxidant, evacuated, sealed, and combusted at 850°C for 12 hrs. The volume of CO_2 quantified during cryogenic distillation was used to calculate organic carbon concentrations in the samples. Carbon isotope abundance in extracted and purified CO_2 was measured with a VG PRISM mass spectrometer at Mountain Mass Spectrometry. To test for the uncertainty of abundance and isotopic composition measurements on TOC, organic-rich and organic-poor standard powders were chosen for replicate (n = 4) analysis. For analyses of the organic-rich sample uncertainties were ± 0.26 mgC/g for abundance (5.57 mgC/g average) and ± 0.03 permil for carbon-isotopic composition (−34.47 permil average); for the organic-poor sample uncertainties were ± 0.06 mgC/g (0.18 mgC/g average) and ± 1.3 permil (−24.1 permil average) for abundance and carbon-isotopic composition, respectively.

Samples chosen for Sr isotopic analysis were treated repeatedly with 0.4 M ammonium acetate (3 times; pH = 8.2) prior to dissolution with 0.5 M acetic acid in order to remove diagenetic components (Gorokhov and others, 1995; Montañez and others, 1996). Strontium was eluted from solution by ion exchange chromatography using ElChrom Sr spec resin and weak 0.05 M nitric acid and measured on a VG Sector 54 multi-collector thermal ionization mass spectrometer at the University of Maryland. Repeated analysis of NBS-987 over a period of 3 months when these samples were analyzed gave a value of 0.710248 +/− 0.000005.

TABLE 1

Sample	$\delta^{13}C$ (PDB)	$\delta^{18}O$ (PDB)	Mineral/ Rock	Ba ppm	Ca %	Fe %	Mg %	Mn %	Sr ppm	Mn/Sr	TOC mgC/g	$\delta^{13}C_{org}$ (PDB)	$\Delta\delta$ (PDB)	$^{87}Sr/^{86}Sr$
Tongwane Formation														
TON/4	2.9	-9.3	Dolomite	14	22.8	2.28	11.9	0.73	47	157	0.09	-28.2	31.1	
TON/5	2.8	-8.8	Dolomite	16	22.68	2.74	11.3	0.64	42	153	0.06	-25.8	28.6	
TON-6	1.9	-9.5	Dolomite					4.7	18	2517				
TON-7A	3.5	-7.1	Dolomite					0.3	24	143				
TON-7B	2.98	-8.26	Dolomite					0.3	29	103				
Duitschland Formation														
Duitschland Farm profile														
Duit/2	-1.3	-14.3	Calcite	< 7	40.17	0.54	0.28	0.14	488	3	0.46	-18.1	16.8	0.712179
Duit/3	-1.8	-14.7	Calcite	< 7	39.43	1.04	0.39	0.21	435	5	0.98	-21.0	19.2	0.713527
Duit/6	-3.1	-10.5	Calcite	< 7	39.91	0.51	0.37	0.10	969	1	1.71	-19.5	16.4	0.711412
Duit/9	-1.4	-12.9	Dolomite	< 7	22.25	4.03	11.2	0.20	127	16	0.31	-21.9	20.5	
Duit/10	-1.6	-11.8	Dolomite	< 7	22.09	3.81	10.8	0.29	137	21	0.27	-18.8	17.2	
Duit/15	6.0	-17.3	Calcite	11	37.27	0.79	0.26	0.18	387	5	0.48	-22.5	28.5	0.704334
Duit/16	6.0	-17.3	Calcite	14	38.25	0.40	0.43	0.19	749	3	0.43	-25.3	31.3	0.704518
Duit/17	5.2	-18.1	Calcite	81	38.07	0.07	1.17	0.25	320	8	0.92	-25.9	31.1	0.712039
Duit/18	4.4	-17.4	Calcite	65	38.37	0.82	0.49	0.29	789	4	0.36	-25.2	29.6	0.708079
Duit/19	8.1	-11.5	Dolomite	8	23.62	0.16	12.8	0.13	49	27	0.40	-26.7	34.8	
Duit/20	7.9	-12.3	Dolomite	37	22.92	0.16	12.9	0.11	39	28	0.35	-26.7	34.6	
Duit/21A	5.5	-18.7	Calcite	12	36.68	0.07	0.50	0.27	141	19	0.36	-24.3	29.8	
Duit/21B	5.6	-18.6	Calcite	22	36.86	0.05	0.50	0.24	137	18	0.31	-24.6	30.2	
Duit/24	2.3	-14.5	Dolomite	< 7	22.81	0.55	13.0	0.14	55	26	0.18	-24.1	26.4	
Duit/25	2.3	-12.2	Dolomite	18	22.83	0.49	13.1	0.09	48	19	0.45	-23.0	25.3	
Duit/26	6.8	-14.9	Dolomite	215	24.40	2.69	11.0	0.12	81	14	0.33	-24.8	31.6	
Duit/28	7.9	-10.7	Dolomite	28	22.97	0.74	12.9	0.12	52	23	0.22	-23.5	31.4	
KB99.3.A			Shale								4.82	-18.7		
KB99.3.B			Shale								3.45	-25.4		
KB99.3.C	-2.0	-14.4	Calcite					0.07	330	2	0.53	-19.0	17.0	
KB99.3.D			Shale								5.6	-26.2		
KB99.3.E			Shale								3.7	-23.5		
KB99.3.F			Shale								3.38	-22.6		
KB99.3.G			Shale								4.09	-24.7		
KB99.3.H			Shale								1.05	-30.6		
KB99.3.I			Shale								1.19	-20.4		
KB99.3.J	6.0	-16.8	Calcite					0.05	612	0.8	0.18	-21.0	27.0	
KB99.3.K	6.0	-16.6	Calcite					0.05	612	0.8	0.22	-22.0	28.0	
KB99.3.L			Shale								0.35	-15.0		
KB99.3.M	6.1	-16.5	Calcite					0.08	645	1.2				
Langbaken Farm profile														
KB99.1.0.5			Shale								3.3	-18.7		
KB99.1.5.0	-1.8	-12.7	Calcite					0.05	318	1.6	0.3	-10.8	9.0	
KB99.1.11.0	-3.0	-9.5	Calcite					0.04	280	1.4	0.4	-14.7	11.3	
KB99.1.19.5	0.1	-10.1	Calcite					0.02	457	0.5	0.5	-14	13.9	
KB99.1.27.5	-2.7	-10.2	Calcite					0.04	307	1.3	1.8	-14.3	11.6	
KB99.1.37.5	-1.8	-10.5	Calcite					0.04	172	2.1	1.4	-12.2	10.4	
KB99.1.60.5	-2.4	-9.1	Dolomite					0.16	44	37.4	0.08	-18.5	16.1	
KB99.1.83.0	-3.7	-9.4	Dolomite					0.24	52	45.7	0.2	-15.2	11.5	
DeHoop Farm profile														
KB99.2.0.5	8.7	-9.4	Dolomite					0.05	57	8.5	0.15	-19.3	28.0	
KB99.2.3.0	9.5	-8.5	Dolomite					0.03	54	4.8	0.08	-17.1	26.6	
KB99.2.4.0	10.1	-6.8	Dolomite					0.02	35	6.0				
KB99.2.9.0	8.9	-10.0	Dolomite					0.04	63	5.6	0.07	-17.7	26.6	
KB99.2.13.5	9.4	-10.9	Dolomite					0.04	95	3.7				
KB99.2.20.0	8.1	-12.1	Dolomite					0.04	70	5.6				
KB99.2.A	2.4	-11.2	Dolomite					0.04	53	7.2				
KB99.2.B	-2.0	-11.9	Calcite					0.03	57	5.2	0.13	-15.2	13.2	
KB99.2.C	2.0	-12.7	Dolomite					0.05	42	11.3	0.08	-19.9	21.9	
Lucknow Formation														
Venn/4	10.3	-8.3	Dolomite					0.02	8.9	21.2	0.33	-25.4	35.7	0.712606
Venn/6	10.5	-7.8	Dolomite					0.02	11.9	19.7	0.22	-24.3	34.8	0.707873

RESULTS

Table 1 includes sample numbers, stratigraphic positions, and analytical results for all samples analyzed in this study. Carbonates in the lower half of the Duitschland Formation are composed of limestone with the exception of dolomite beds immediately below the sequence boundary. Carbonates above this boundary consist of both limestone and dolomite with the latter increasing upsection. Calculations based on yields of carbon dioxide from reaction with phosphoric acid indicated that the carbonate content in most samples exceeded 70 percent.

Elemental analyses reveal that limestone samples are significantly enriched in strontium (up to 969 ppm) relative to dolomites in the Duitschland Formation (table 1; see also Martini, 1979). Manganese concentration in the Duitschland carbonates is quite variable. This results in Mn/Sr (a common diagenetic indicator for marine carbonates; for example, Veizer, 1983; Derry, Kaufman, and Jacobsen, 1992; Kaufman, Knoll, and Awramik, 1992) ranging from 1 to 28, with the highest values in limestone samples adjacent to the two mafic sills, as well as in all dolomites.

Oxygen isotope values for Duitschland carbonates from the type section at Duitschland Farm are notably lower than −10 permil, suggesting exchange of the oxygen in primary carbonates with hot fluids, likely associated with Bushveld intrusion (Valley, 1986). Sampled localities that are farther away from this large igneous province (Langbaken and DeHoop) contain equivalent carbonates less depleted in ^{18}O (table 1).

All carbonates in the lower part of the Duitschland Formation are depleted in ^{13}C with a minimum value of −3.7 permil. In strong contrast, most carbonates above the sequence boundary are systematically enriched in ^{13}C with a maximum value of +10.1 permil. However, in the upper part of the formation above a second diamictite level $\delta^{13}C$ values are consistently lower; on DeHoop Farm a single sample of flat laminated cherty limestone has a value of −2 permil. Notably, limestone samples adjacent to the mafic sills are 2 to 4 permil less enriched in ^{13}C relative to nearby dolomites.

Total organic carbon (TOC) isolated from shale and carbonate samples range in abundance between 0.06 and 5.6 mgC/g sample. These organic isolates have variable $\delta^{13}C$ values (ranging between −30.6 to −10.8 permil), with carbonates being consistently more ^{13}C enriched than interbedded shales. The $\delta^{13}C$ values of organic isolates from carbonates of the upper Duitschland range between −26.7 to −15.0 permil.

Six samples were selected for Sr isotope analysis based on their Sr abundances (>300 ppm) and Mn/Sr ratios (< 5; table 1). Two closely spaced samples from the level of the isopachous sheet cements in the upper half of the Duitschland Formation yielded similarly low $^{87}Sr/^{86}Sr$ values (about 0.7043-0.7045); other analyzed samples were considerably more radiogenic.

EFFECTS OF DIAGENESIS AND METAMORPHISM

In any geochemical consideration of sedimentary rocks, post-depositional effects on primary elemental and isotopic compositions must be considered. Post-depositional processes may result in the alteration of marine carbonates, which can be recognized through a detailed study of elemental and isotopic trends (Veizer, 1983; Fairchild, Marshall, and Bertrand-Sarfati, 1990; Banner and Hanson, 1990; Derry, Kaufman, and Jacobsen, 1992; Jacobsen and Kaufman, 1999). Superimposed on regional insults, the diagenetic picture for the Duitschland Formation is complicated by the intrusion in the type area of mafic sills into the upper part of the formation.

Because of the predominance of oxygen in all fluids, the oxygen isotopic compositions of carbonates are substantially altered before carbon isotope values under the influence of meteoric or hydrothermal solutions. Lower $\delta^{18}O$ values commonly indicate a higher degree of exchange between post-depositional fluids and carbonates. Oxygen isotope values of studied carbonates are approx −10 permil or less in most

samples, with a greater degree of ^{18}O depletion noted at Duitschland Farm. It is clear that the oxygen isotope composition of all samples has been altered to some degree, although the most enriched values (up to −6.8 permil) are consistent with those found in well-preserved Paleoproterozoic successions worldwide (Veizer, Clayton, and Hinton, 1992; Veizer and others, 1992; Melezhik, Fallick, and Clark, 1997; and our own unpublished data). In the upper half of the formation, limestones adjacent to the mafic sills have the most ^{18}O depleted compositions (see Valley, 1986 for the effects of contact metamorphism on both O and C isotopes in carbonates); however, nearby dolomites are notably more enriched in ^{18}O, similar to carbonates in the lower half of the formation. Carbonates analyzed by Buick and others (1998) were specifically collected near these mafic sills.

Mn/Sr elemental ratios are also used as an indicator of postdepositional alteration in carbonates (Veizer, 1983), where higher Mn and lower Sr abundance are typically related to meteoric diagenesis. Application of these criteria is rather ambiguous to Paleoproterozoic carbonates that may have formed in an anoxic ocean enriched in Fe^{2+} and Mn^{2+}. As expected due to crystal lattice effects, Sr contents are higher and Mn/Sr ratios are much lower in calcites than in dolomites (table 1). Low Sr concentrations in dolomites (up to 140 ppm) may be localized in fluid or mineral inclusions (Veizer, 1983).

Because Sr is a trace element in carbonate, $^{87}Sr/^{86}Sr$ ratios are easily altered through exchange with radiogenic fluids of continental derivation or the *in situ* decay of ^{87}Rb to ^{87}Sr in clay and clastic minerals within the carbonates. Strontium isotope ratios were measured in samples with low Mn/Sr and high Sr concentrations. All analyzed samples from the lower part of succession, regardless of their present Sr contents, have highly radiogenic Sr isotope values (table 1). This is likely the consequence of the interbedding of these relatively thin limestone horizons in a predominantly shaley interval. On the other hand, two closely spaced samples from thick carbonates with isopachous cements and relatively high Sr contents in the upper part of the succession (Duit/15 and Duit/16) had virtually the same $^{87}Sr/^{86}Sr$ value. We tentatively interpret these low values (about 0.7045) as reflecting ocean $^{87}Sr/^{86}Sr$ values around 2.4 Ga ago.

Carbon isotope exchange between co-existing organic matter and carbonates during metamorphism may lead to a depletion of ^{13}C in carbonates and enrichment of ^{13}C in organic C (Valley, 1986), resulting in lower $\Delta\delta$ values. In this study, however, we note no relationship between TOC contents and $\delta^{13}C$ values of organic matter that might result from regional metamorphism (Hayes, Kaplan, and Wedeking, 1983). The degree of carbon isotope fractionation varies throughout the succession with an apparent bimodal stratigraphic distribution of values. In the underlying Tongwane Formation and all but one Duitschland sample above the sequence boundary, $\Delta\delta$ values range between 21.9 and 34.8 permil with an average of about 30 permil. These values are comparable with those found in 2.2 to 2.1 Ga carbonates of the Fennoscandian Shield (Karhu, 1993) and with the long-term average of around 30 permil for the last 800 Ma (Hayes, Strauss, and Kaufman, 1999). These values are consistent with maximal carbon isotope fractionations by primary producers in the ocean and further suggest that the upper Duitschland carbonates were not strongly affected by postdepositional processes, including contact metamorphism.

On the other hand, samples below the sequence boundary have negative $\delta^{13}C$ in carbonates containing organic matter significantly enriched in ^{13}C (resulting in smaller $\Delta\delta$ values) ranging between 9.0 and 20.5 permil. A similarly low $\Delta\delta$ value is recorded in the single anomalous limestone sample above the sequence boundary, which notably lies immediately above a diamictite of unknown origin at ~850 m (fig. 5). Both negative $\delta^{13}C$ values and a smaller magnitude of carbon isotope fractionation

might be explained by metamorphic equilibration. This interpretation, however, conflicts with a similarity in $\delta^{18}O$ values throughout the succession. The higher abundance of TOC in the lower part of the formation as well as the larger $\Delta\delta$ in the contact metamorphosed upper part of the formation is also inconsistent with a higher metamorphic grade for lower Duitschland sedimentary rocks. Analyses of organic-rich Neoproterozoic "cap carbonates" in Namibia and the United States of America also show significantly reduced $\Delta\delta$ values (Kaufman, Hoffman, and Halverson, 1997; Hayes, Strauss, and Kaufman, 1999) similar to those reported here from the lower Duitschland carbonates. If the smaller $\Delta\delta$ values are not a post-depositional phenomenon, then it is conceivable that the reduced fractionation is due to carbon limitation to growing cells in shallow seawater. Two environmental options seem viable: (1) either carbon dioxide was limiting because of low concentrations in the atmosphere (Jasper and Hayes, 1990; Freeman and Hayes, 1991), or (2) high growth rates resulted in a depletion of intracellular CO_2 available for fixation (Bidigare and others, 1997, 1999; Popp and others, 1998). Based on experience from the Neoproterozoic record, the combined organic and inorganic carbon isotope results from the organic-rich lower Duitschland sedimentary rocks suggest deposition in the immediate aftermath of a global glaciation (see discussion below).

In conclusion, most of the samples in this study appear to record near to primary carbon isotope compositions in both organic and inorganic phases. While two closely spaced samples also appear to preserve unaltered $^{87}Sr/^{86}Sr$ values, most are likely reset. All oxygen isotope compositions of Duitschland carbonates appear to be reset to variable degrees.

The relationship of isotope anomalies and ice ages in the Transvaal basin

Assuming that little-altered carbon isotope compositions are preserved in the Duitschland Formation carbonates, we can now ask about the stratigraphic relationship of carbon isotope anomalies and glacial phenomena. The only unequivocal glacial horizon previously recognized in the Transvaal basin occurs within the upper Timeball Hill Formation (fig. 3). The notable ^{13}C enrichment of upper Duitschland carbonates (along with co-existing organic matter) stratigraphically beneath the glacial deposits supports the view that at least one Paleoproterozoic ice age was preceded by a positive carbon isotope anomaly. Lacking absolute age constraints, however, the time between deposition of upper Duitschland carbonates and the Timeball Hill diamictite is unknown.

Above the Makganyene Diamictite, the equivalent of the upper Timeball Hill diamictite in the Griqualand West basin, are finely-laminated carbonate-bearing manganese ores of the Hotazel Formation (Beukes, 1983; Tsikos and Moore, 1997). This sedimentary ore deposit is suggested to have accumulated in the aftermath of a widespread and potentially global glaciation (Kirschvink and others, 2000). During this ice age Fe and Mn apparently built up to high concentrations in an anoxic ocean dominated by hydrothermal inputs. These deep water manganese-rich carbonates have highly negative $\delta^{13}C$ values (ranging between -12 to -15 permil), which Kirschvink and others (2000) interpret as a syn-sedimentary overprint of recycled organic matter on primary ocean compositions nearer to -5 permil (Calver, 2000). Notable accumulations of carbonate hosted Mn ore are known in ^{13}C-depleted Neoproterozoic cap rocks from China (Li and others, 1999), Brazil (Urban, Stribrny, and Lippolt, 1993), and Namibia (Bühn, Stanistreet, and Okrusch, 1992).

Above the diamictite and the Hotazel cap rock are dolomites of the Mooidraai Formation, which have $\delta^{13}C$ values near to 0 permil (Bau and others, 1999; Kirschvink and others, 2000). Unconformably overlying the Mooidraai Formation is the Mapedi Shale and the Lucknow Formation of the Olifantshoek Group (fig. 3). Highly ^{13}C-enriched carbonates of the Lucknow Formation have been considered as evidence for

a post-2.1 Ga carbon isotope excursion, based on the 1928±4 Ma Pb-Pb zircon age of the overlying Hartley Basalt (Buick and others, 1998; Melezhik and others, 1999). This interpretation, however, is inconsistent with field observations of unconformity between the Lucknow Formation and Hartley basalts (fig. 3; Swart, ms; Dorland, ms), as well as new litho- and chemo-stratigraphic correlations between the lower part of the Olifantshoek Group and the upper part of the Pretoria Group, which is intruded by the ~2.06 Ga old Bushveld Complex (Beukes and others, 2001). The Lucknow and equivalent Silverton formations in South Africa and the Lomugundi Formation in Zimbabwe all contain carbonates highly enriched in ^{13}C (> +10 permil; Schidlowski, Eichmann, and Junge, 1976; Master and others, 1993; Buick and others, 1998; see additional data in table 1). Given their stratigraphic position above glacial strata and beneath the 2.06 Ga Bushveld felsites, the biogeochemical anomaly preserved at this stratigraphic level may be equivalent to the ca. 2.1 to 2.2 Ga event described by Karhu and Holland (1996).

As discussed above, carbonates in the lower Duitschland Formation have negative $\delta^{13}C$ values, and lie above a diamictite recently established to be glacial in origin (Coetzee, ms; Beukes and others, 2001). Lower Duitschland carbonates occur within a 400 m sequence beginning with deep-water facies and shallowing upward to the first clear sequence boundary at approx 400 m (fig. 5). This stratigraphic framework is strikingly similar to post-glacial carbonate-dominated sequences in the Neoproterozoic of Namibia (Hoffman, Kaufman, and Halverson, 1998; Hoffman and others, 1998). These thick (up to 500 m) finely-laminated and stromatolitic cap carbonates, which conformably overlie diamictites, were deposited below the storm-wave base, lack exposure surfaces, and shallow to sealevel only in their upper parts (Kaufman, Knoll, and Narbonne, 1997; Hoffman, Kaufman, and Halverson, 1998; Hoffman and others, 1998). Due to the lack of exposure surfaces in both Neoproterozoic and Paleoproterozoic examples, it is conceivable that the accommodation space – later filled by several hundred meters of sediment – was created by subsidence on continental margins during extended glaciation (Hoffman, Kaufman, and Halverson, 1998).

Unconformably below the lower Duitschland diamictite are carbonates of the Tongwane Formation, which have only moderately enriched carbon isotope values (about +3.5 permil, table 1), and the Penge Iron Formation. At present there are no known carbonates beneath this diamictite with strongly positive $\delta^{13}C$ values. This might be due to missing stratigraphy beneath the unconformity surface, but we note that carbonates sandwiched between early Paleoproterozoic glacial strata and banded iron-formations worldwide are not significantly enriched in ^{13}C. Beneath the Penge Iron Formation, platform carbonates of the Malmani Subgroup and equivalents have $\delta^{13}C$ values very close to 0 permil (Beukes and others, 1990; Veizer, Clayton, and Hinton, 1992).

Summarizing data from the Transvaal Basin and equivalents, there now appears to be compelling lithologic and biogeochemical evidence for at least two Paleoproterozoic ice ages in South Africa. Given this discovery, we then ask how might these two events correlate with the three known levels glaciations preserved in the Huronian Supergroup of North America?

CORRELATION WITH THE HURONIAN SUPERGROUP

The three levels of glacial deposits in the Paleoproterozoic Huronian Supergroup include, from youngest to oldest, the Gowganda, Bruce, and Ramsay Lake Formations. Carbonates, however, only occur at two levels in the Huronian stratigraphy. The Gordon Lake Formation, which is stratigraphically above the youngest diamictite but older than the 2.22 Ga Nipissing sills that intrude the whole succession, has carbonates with highly positive $\delta^{13}C$ (up to +8 permil) values (Bekker, Karhu, and Bennett, 1996). The Espanola Formation rhythmites, which sit immediately above the Bruce diamic-

tite, are characterized by negative $\delta^{13}C$ values (Veizer, Clayton, and Hinton, 1992) and are interpreted here as a cap carbonate. Negative $\delta^{13}C$ values are also noted in equivalent carbonates atop the middle of three diamictite horizons in the Paleoproterozoic Snowy Pass Supergroup (Bekker and Karhu, 1996; Bekker and others, 1999).

Clearly the lack of carbonate lithologies complicates chemostratigraphic correlation with units in South Africa. Nonetheless, it seems plausible that the uppermost Huronian glacial unit is correlative with the Upper Timeball Hill Formation diamictite and equivalents. This tentative correlation is based on the position of these glacial deposits beneath highly ^{13}C enriched carbonates (the Gordon Lake and Silverton/Lucknow formations in Canada and South Africa, respectively) and oxygenated paleosols, aluminous shales, and mature quartzites (Young, 1973; Rainbird, Nesbitt, and Donaldson, 1990; Beukes, Gutzmer, and Dorland, 1999; Gutzmer and Beukes, 1996; Schreiber and Eriksson, 1992).

Correlation of lower Duitschland cap carbonate facies with Espanola rhythmites is tempting, but lacking independent chronostratigraphic constraints it remains uncertain whether the lower Duitschland diamictite is equivalent to the Bruce or Ramsay Lake formations in the Huronian succession.

A Paleoproterozoic Snowball Earth?

The Neoproterozoic Snowball Earth hypothesis suggests that the planet was blanketed by continental glaciers and sea ice, extending to equatorial latitudes, for several million years (Hoffman and others, 1998). During such a catastrophic event the photosynthetic, hydrologic, and weathering cycles would have been shut down while the ocean quickly became anoxic and dominated by hydrothermal inputs. To escape from the extreme albedo of an ice-covered planet, CO_2 concentrations must have built up to phenomenal levels through millions of years of volcanic inputs (Caldiera and Kasting, 1992). The drawdown of atmospheric CO_2 levels resulting in an icehouse climate has been plausibly linked to the fragmentation of the Rodinia. By increasing the length of continental margins, breakup of the supercontinent resulted in the creation of a larger repository for organic matter. Enhanced biological productivity and an increase in the proportional burial of organic carbon over these passive margins, stimulated by higher concentrations of key nutrients in the Proterozoic oceans, is expressed in the highly positive $\delta^{13}C$ values of carbonate deposited prior to the glacial diamictites (Kaufman and Knoll, 1995; Kaufman, Knoll, and Narbonne, 1997).

Given that recent paleomagnetic results suggest equatorial glaciation in the Paleoproterozoic, we now ask whether similar tectonic and environmental changes bracket these ancient ice ages? Tectonic reconstruction and available age constraints indicate that the Paleoproterozoic supercontinent Kenoraland began rifting around 2.45 Ga (Williams and others, 1991; Heaman, 1997) prior to the ice ages. It is believed that rifting resulted in a high hydrothermal flux of Fe to the oceans and the deposition of BIFs worldwide (Beukes and others, 1990; Barley, Pickard, and Silvester, 1997). Subsidence over millions of years of global glaciation may be related to the creation of large accommodation space filled up by lower Duitschland sediments in the aftermath of global glaciation. A buildup of Fe and Mn concentrations in the deep anoxic ocean beneath the global ice pack over millions of years is also inferred from the deposition of the manganiferous Hotazel Formation above the equivalent of Timeball Hill glacial strata (Kirschvink and others, 2000).

The hypothesis that the anoxic glacial oceans were dominated by hydrothermal inputs, which included key biolimiting nutrients like iron (Coale and others, 1996; Falkowski, Barber, and Smetacek, 1998) and phosphorous (van Cappellan and Ingall, 1994), may provide a clue to the reduced $\Delta\delta$ values measured in the organic-rich rocks of the lower Duitschland Formation. Since low pCO_2 is unlikely in the aftermath of a

Snowball Earth (Caldiera and Kasting, 1992), carbon limitation through extreme growth rates of photoautotrophs is the most likely process resulting in the markedly decreased carbon isotope fractionations (Kaufman, Hoffman, and Halverson, 1997). Under conditions where nutrients are readily available, the rate of carbon fixation within cells can be faster than the rate of diffusion of dissolved CO_2 into the cells (Berry, 1988; Riebesell, Wolf-Gladrow, and Smetacek, 1993; Bidigare and others, 1997), which in part may be related to cell geometry (Popp and others, 1998). This would result in less isotopic discrimination and enrichment of ^{13}C in biomass. This view is strongly supported by recent experiments conducted during the IronEx II iron fertilization of the low productivity equatorial Pacific Ocean (Bidigare and others, 1999). These authors report up to a 7 permil carbon isotopic enrichment in algal biomass, which is largely the result of elevated growth rates. In addition to the carbon isotopic enrichment and significantly reduced $\Delta\delta$, stimulation of growth rate was accompanied by a seven-fold increase in the export of particulate organic carbon to sediments.

Finally, if high pCO_2 lasted for some time after the ice age, it is likely that high temperature and high weathering rates in stable tectonic environment would have resulted in lateritic paleosols and mature quartzites in overlying units. Evidence for these lithologies, unusual in the context of successions otherwise dominated by immature siliciclastics, are preserved immediately above the youngest Paleoproterozoic diamictites in North America, Fennoscandia, and South Africa (Young, 1973; Gutzmer and Beukes, 1996; Schreiber and Eriksson, 1992; Marmo, 1992).

Speculation on the Timing of Paleoproterozoic Atmospheric Oxygen Rise

The composition of Earth's Archean and Paleoproterozoic atmosphere is at the heart of a heated controversy between researchers who maintain that surface environments were either oxidizing from the origin of oxygenic photosynthesis onward (Ohmoto, 1997) or were near-neutral until a critical oxygenation event around 2 by ago (Holland, 1994; Rye and Holland, 1998). In the latter model, atmospheric pO_2 was likely below 0.1 percent PAL until tectonic and biological forces resulted in an oxygen buildup to 15 percent or greater. In the rock record, evidence of this event is marked by (1) the retention of iron in fossil soil horizons; (2) the apparent cessation of detrital uraninite and pyrite deposits as well as banded iron-formations; and (3) the sudden appearance of sedimentary red beds. Recently, the late Paleoproterozoic oxidation event was tied to extraordinary changes in the carbon isotope composition of marine carbonates (Karhu and Holland, 1996) and organic matter (Des Marais and others, 1992; Des Marais, 1997), potentially linked to the enhanced proportional burial of organic matter in sediments deposited between 2.2 to 2.1 Ga.

Following the interpretation of strong positive $\delta^{13}C$ anomalies as markers of oxidation events (Broecker, 1970; Hayes, 1983; Derry, Kaufman, and Jacobsen, 1992; Kaufman and Knoll, 1995; Karhu and Holland, 1996; Kaufman, Knoll, and Narbonne, 1997; but see Kump and others, 1999 for contrary view) suggests that the Paleoproterozoic oxygen buildup may have started up to 200 my earlier during deposition of the upper Duitschland beds. Of the factors believed to result in the enhanced burial of organic carbon and extreme ^{13}C enrichment of surfical seawater, those that appear to be most important are (1) high sedimentation rates, (2) bottom water anoxia, and (3) high biological productivity (Pedersen and Calvert, 1990). Unfortunately, the lack of a continuous record of Sr isotope changes in Paleoproterozoic oceans makes it difficult to estimate rates of continental erosion and sedimentation.

Support for an earlier oxygenation event comes from new field evidence for an oxidized 2.4 Ga paleosol and red beds of similar age in South Africa (Beukes, Gutzmer, and Dorland, 1999). In contrast, geochemical analyses of incomplete sections of the Hekpoort basalt were previously used to infer anoxic environment during their

formation (Holland, 1994; Rye and Holland, 1998). Red beds were recently discovered in the basal part of the Timeball Hill Formation below the diamictite (Beukes, Gutzmer, and Dorland, 1999). Timeball Hill beds are also unique because they contain the oldest sulfide minerals whose range of S-isotopic compositions suggests a buildup of oxidants in the ocean used by sulfate-reducing microbial communities (Cameron, 1982). Additionally, a strong negative Ce anomaly is preserved in Timeball Hill shales (Reczko, Eriksson, and Snyman, 1995) as well as the broadly equivalent manganiferous carbonates of the Hotazel Formation (Bau and others, 1999). It is significant that no Ce anomaly is present in older metalliferous sedimentary rocks of the Penge Iron-Formation and equivalents in the Griqualand West Basin (Bau and others, 1999). Notably, in Botswana equivalents of the Rooihoogte Formation, presently considered to be time-equivalent to the upper Duitschland Formation (Swart, ms; fig. 4), contain manganese-rich stromatolitic dolomite and banded ironstone (Steyn, Gardyne, and Klop, 1986). These may represent the oldest Mn-rich deposits associated with the oxygenation of Earth's surface environment in the aftermath of one of the oldest ice ages.

In Canada, the oldest red and variegated beds occur in the pre-2.22 Ga Gowganda Formation of the Huronian Supergroup (Wood, 1979; Rainbird and Donaldson, 1988), again closely associated with glacial deposits and oxidized paleosols (Rainbird, Nesbitt, and Donaldson, 1990). The initial increase in sulfur isotope fractionation is recorded in beds immediately overlying the Gowganda Formation (Hattori, Krouse, and Campbell, 1983).

In Paleoproterozoic sedimentary rocks of Australia and elsewhere, paleontological and biomarker studies indicate the presence of oxygenic photoautotrophs as well as eukaryotes as old as 2.7 Ga (Summons and others, 1999; Brocks and others, 1999). It is possible, however, that these microorganisms evolved in local environments before the atmosphere and hydrosphere became fully oxygenated. Lastly, the discovery of mass-independent sulfur isotope fractionations in early Paleoproterozoic sedimentary sulfates and sulfides – theoretically linked to photochemical reactions in an ozone-depleted atmosphere (Farquhar and others, 2000) – support the view of an earlier, approx 2.4 Ga ago, rise in oxygen.

It is likely that atmospheric oxygen levels continued to rise from the time of upper Duitschland deposition through the extreme biogeochemical anomaly around 2.1 to 2.2 Ga (Karhu and Holland, 1996). However, if surface oxidation was tied to modulation in the organic carbon burial flux (Des Marais and others, 1992; Derry, Kaufman, and Jacobsen, 1992; Kaufman, Jacobsen, and Knoll, 1993; Des Marais, 1997) atmospheric oxygen contents may have similarly oscillated through this interval. The reappearance of a large province of 2.1 to 1.9 Ga sedimentary iron formation in strata above equivalents of Huronian beds (Isley, 1995; Simonson and Hassler, 1996) suggests that the deep ocean was not irreversibly oxidized, even after the carbon isotope event described by Karhu and Holland (1996). In sum, the lithologic and geochemical data tied to new age constraints from South Africa suggest that the oxygen content of the Paleoproterozoic atmosphere oscillated accordingly to changes in the carbon cycle, perhaps closely associated with biological and tectonic events.

CONCLUSIONS

As demonstrated here, the emerging temporal pattern of Paleoproterozoic carbon isotope variations and glaciation has a close analogue to Neoproterozoic events, suggesting a coupling of climatic and biogeochemical changes at either end of the eon. In both intervals a marked decrease in atmospheric CO_2 levels, either through high productivity and burial of organic carbon (Kaufman, Knoll, and Narbonne, 1997) or by intense weathering (Hoffman and Schrag, 2000), may have resulted in global glaciation (Hoffman and others, 1998). In the context of the Proterozoic Eon as a

whole however, it is notable that the intervening Mesoproterozoic (1.0-1.7 Ga) interval lacks evidence of glaciation or of extreme $\delta^{13}C$ excursions (Buick, Des Marais, and Knoll, 1995; Knoll, Kaufman, and Semikhatov, 1995; Brasier and Lindsay, 1998; Kah and others, 1999). Furthermore, there are some unresolved differences between Neoproterozoic and Paleoproterozoic $\delta^{13}C$ excursions and environmental perturbations. Contrary to prediction (Kaufman, 1997), there is no known significant ^{13}C enrichment in carbonate unit below the Duitschland diamictite and above the Penge Iron Formation and potential equivalents worldwide. Similarly, the end of the Paleoproterozoic carbon isotope excursion at approx 2.1 Ga is not marked by recognized glacial phenomenon. While these discrepancies might be the result of omissions in these truly ancient stratigraphic records, they might also be real. In either case they warrant further investigation.

ACKNOWLEDGEMENTS

The authors wish to thank Jim Wright at Rutgers University, Dan Schrag at Harvard University, and Matt Emmons at Mountain Mass Spectrometry for additional stable isotope analyses as well as Phil Candela and Richard Walker at the University of Maryland for access to geochemical facilities. Support for AJK came from NSF grant EAR-96-14070. The Open Research Program of the National Research Foundation in Pretoria, South Africa provided support for NJB. The Geological Survey of Finland is thanked by JK for permission to publish data produced in their laboratories. The Virginia Polytechnical Institute and grants from the Geological Society of America supported AB during this project. Lastly, we thank David Des Marais and Lee Kump for thoughtful and constructive reviews.

APPENDIX 1

Sample description, locality, and stratigraphic position in respect to the marker beds. Heights of samples in meters above the base of the Duitschland Formation are given for samples collected at Duitschland Farm, as well as estimated heights for correlative sections at Langbaken (KB99.1 series) and de Hoop (KB99.2 series) farms. Samples of the Tongwane Formation were collected in the Tongwane riverbed, just below the Duitschland Formation (see fig. 4).

Sample	Position of sample in unit	Sample description
Tongwane Formation		
TON/4		Argillaceous massive dolomite
TON/5		Argillaceous massive dolomite
TON/6		Argillaceous massive dolomite
TON/7A		Nodule from nodular dolomite
TON/7B		Matrix from nodular dolomite
Duitschland Formation		
Duitschland Farm profile		
Duit/2	280	Flat-laminated light-gray algal limestone
Duit/3	300	Flat-laminated limestone clast within a clay matrix
Duit/6	325	Slightly dolomitized flat-laminated limestone
Duit/9	380	Light-gray massive dolomite with stylolites
Duit/10	390	Light-gray massive dolomite with stylolites and cryptic stromatolites
Duit/15	680	Light-gray limestone with flat laminations and columnar stromatolites
Duit/16	690	Light-gray limestone with flat laminations and columnar stromatolites
Duit/17	700	Flat-laminated gray limestone with slight dolomitization and recrystallization
Duit/18	740	Light-gray oolitic limestone with slight metamorphism
Duit/19	745	Flat-laminated gray limestone with stratiform stromatolites
Duit/20	755	Light-gray oolitic limestone
Duit/21A	765	Gray limestone with pink discolouration due to recrystallization
Duit/21B	765	Gray limestone with pink discolouration due to recrystallization
Duit/24	860	White leached and recrystallized dolomite with domal stromatolites

Appendix 1

(continued)

Duit/25	870	White leached and recrystallized dolomite with domal stromatolites
Duit/26	925	Argillaceous dolomite with stratiform stromatolites
Duit/28	950	Massive recrystallized dolomite with chertification and karst breccia
KB99.3.A	245	Black shale
KB99.3.B	260	Black shale
KB99.3.C	300	Limestone clast within a clay matrix
KB99.3.D	325	Shale
KB99.3.E	345	Black shale
KB99.3.F	360	Black shale
KB99.3.G	375	Black shale
KB99.3.H	400	Gray shale
KB99.3.I	445	Gray shale
KB99.3.J	680	Isopachous sheet cements (limestone). Inorganic precipitates
KB99.3.K	695	Laminated limestone with chert
KB99.3.L	705	Gray shale
KB99.3.M	715	Isopachous sheet cements (limestone). Inorganic precipitates
Langbaken Farm profile		
KB99.1.0.5	280	Interbedded limestone and shale
KB99.1.5.0	285	Laminated limestone
KB99.1.11.0	295	Laminated limestone
KB99.1.19.5	305	Laminated limestone
KB99.1.27.5	325	Laminated limestone
KB99.1.37.5	335	Laminated limestone
KB99.1.60.5	360	Laminated dolomite
KB99.1.83.0	385	Thin dolomite in marly unit
DeHoop Farm profile		
KB99.2.0.5	960	Silicified stromatolitic dolomite
KB99.2.3.0	957	Silicified stromatolitic dolomite

Appendix 1

(continued)

KB99.2.4.0	956	Silicified stromatolitic dolomite
KB99.2.9.0	951	Dolomite
KB99.2.13.5	946	Dolomite
KB99.2.20.0	938	Marl/Dolomite
KB99.2.A	880	Dolomite
KB99.2.B	875	Flat-laminated cherty limestone
KB99.2.C	868	Stromatolitic dolomite above breccia
Lucknow Formation		
Venn/4		Brown/pink fine-grained dolomitic mudstone
Venn/6		Brown/pink fine-grained dolomitic mudstone

References

Altermann, W., and Nelson, D. R., 1998, Sedimentation rates, basin analyses, and regional correlations of three Neoarchaean and Paleoproterozoic sub-basins of the Kaapvaal Craton as implied by precise SHRIMP U-Pb zircon ages from volcanic sediments: Journal of Sedimentary Geology, v. 120, p. 225–256.

Baker, A. J., and Fallick, A. E., 1989, Evidence from Lewisian limestones for isotopically heavy carbon in two-thousand-million-year-old sea water: Nature, v. 337, p. 352–354.

Banner, J. L., and Hanson, G. N., 1990, Calculation of simultaneous isotopic and trace element variations during water-rock interaction with application to carbonate diagenesis: Geochimica et Cosmochimica Acta, v. 54, p. 3123–3137.

Barley, M. E., Pickard, A. L., and Silvester, P. J., 1997, Emplacement of a large igneous province as a possible cause of banded iron formation 2.45 billion years ago: Nature, v. 385, p. 55–58.

Bau, M., Romer, R. L., Lüders, V., and Beukes, N. J., 1999, Pb, O, and C isotopes in silicified Mooidraai dolomite (Transvaal Supergroup, South Africa): implications for the composition of Paleoproterozoic seawater and 'dating' the increase of oxygen in the Precambrian atmosphere: Earth and Planetary Science Letters, v. 174, p. 43–57.

Bekker, A., Eriksson, K. A., Kaufman, A. J., Karhu, J. A., and Beukes, N. J., 1999, Paleoproterozoic record of biogeochemical events and ice ages: Geological Society of America, Annual Meeting, Abstracts with Programs, v. 31, no. 7, p. A-487.

Bekker, A., and Karhu, J. A., 1996, Study of carbon isotope ratios in carbonates of the Early Proterozoic Snowy Pass Supergroup, WY and its application for correlation with the Chocolay Group, MI and Huronian Supergroup, ON [abstract]: Institute on Lake Superior Geology, 42nd Annual Meeting, Cable, Wisconsin, 1996, Proceedings, v. 42, part 1, p. 4–5.

Bekker, A., Karhu, J. A., and Bennett, G., 1996, Lomagundi event in North America: application for stratigraphic correlation: Geological Society of America, Annual Meeting, Abstracts with Programs, v. 28, no. 7, p. A-229.

Berry, J. A., 1988, Studies of mechanisms affecting the fractionation of carbon isotopes in photosynthesis, *in* Ehleringer, J. R., and Nagy, K. A., editors, Stable isotopes in Ecological Research: New York, Springer-Verlag, p. 82–94.

Beukes, N. J., 1983, Paleoenvironmental setting of iron-formations in the depositional basin of the Transvaal Supergroup, South Africa, *in* Trendall, A. F., and Morris, R. C., editors, Iron-formations: Facts and problems: Amsterdam, Elsevier, p. 131–209.

Beukes, N. J., Bekker, A., Swart, Q., Dorland, H., Van Niekerk, H. S., Gutzmer, J., Karhu, J. A., and Kaufman, A. J., 2001, Implications of carbon isotope values of South African carbonates for the Paleoproterozoic secular carbon isotope curve: European Union of Geoscientists, Abstract Supplement, v. 13, no. 1, p. 88.

Beukes, N. J., Gutzmer, J., and Dorland, H., 1999, Paleoproterozoic laterites, supergene iron and manganese ores and atmospheric oxygen: Geological Society of Australia Abstracts, p. 20–23.

Beukes, N. J., Klein, C., Kaufman, A. J., and Hayes, J. M., 1990, Carbonate petrology, kerogen distribution, and carbon and oxygen isotope variations in an Early Proterozoic transition from limestone to iron-formation deposition, Transvaal Supergroup, South Africa: Economic Geology, v. 85, p. 663–690.

Bidigare, R. R., and 14 others, 1997, Consistent fractionation of ^{13}C in nature and in the laboratory: Growth rate effects in some haptophyte algae: Global Biogeochemical Cycles, v. 11, p. 279–292.

Bidigare, R. R., and 11 others, 1999, Iron-stimulated changes in ^{13}C fractionation and export by equatorial Pacific phytoplankton: Toward a paleogrowth rate proxy: Paleoceanography, v. 14, p. 589–595.
Brasier, M. D., and Lindsay, J. F., 1998, A billion years of environmental stability and the emergence of eukaryotes: New data from northern Australia: Geology, v. 26, p. 555–558.
Brocks, J. J., Logan, G. A., Buick, R., and Summons, R. E., 1999, Archean molecular fossils and the early rise of eukaryotes: Science, v. 285, p. 1033–1036.
Broecker, W. S., 1970, A boundary condition of the evolution of atmospheric oxygen: Journal of Geophysical Research, v. 75, p. 3553–3557.
Buchan, K. L., Mortensen, J. K., Card, K. D., and Percival, J. A., 1998, Paleomagnetism and U-Pb geochronology of diabase dyke swarms of Minto block, Superior Province, Quebec, Canada: Canadian Journal of Earth Sciences, v. 35, p. 1054–1069.
Bühn, B., Stanistreet, I. G., and Okrusch, M., 1992, Late Proterozoic outer shelf manganese and iron deposits at Otjosondu (Namibia) related to the Damaran oceanic opening: Economic Geology, v. 87, p. 1393–1411.
Buick, I. S., Uken, R., Gibson, R. L., and Wallmach, T., 1998, High-$\delta^{13}C$ Paleopoterozoic carbonates from the Transvaal Supergroup, South Africa: Geology, v. 26, p. 875–878.
Buick, R., Des Marais, D. J., and Knoll, A. H., 1995, Stable isotopic compositions of carbonates from the Mesoproterozoic Bangemall Group, northwestern Australia: Chemical Geology, v. 123, p. 153–171.
Button, A., 1986, The Transvaal sub-basin of the Transvaal sequence, *in* Anhaeusser, C. R., and Maske, S., editors, Mineral deposits of Southern Africa, v. 1: Johannesburg, Geological Society of South Africa, p. 811–817.
Caldeira, K., and Kasting, J. F., 1992, Susceptibility of the early Earth to irreversible glaciation caused by carbon dioxide clouds: Nature, v. 359, p. 226–228.
Calver, C. R., 2000, Isotope stratigraphy of the Ediacarian (Neoproterozoic III) of the Adelaide Rift Complex, Australia, and the overprint of water column stratification: Precambrian Research, v. 100, p. 121–150.
Cameron, E. M., 1982, Sulphate and sulphate reduction in early Precambrian oceans: Nature, v. 296, p. 145–148.
Cheney, E. S., and Twist, D., 1991, The conformable emplacement of the Bushveld mafic rocks along a regional unconformity in the Transvaal succession of South Africa: Precambrian Research, v. 52, p. 115–132.
Coale, K. H., and 18 others, 1996, A massive phytoplankton bloom induced by an ecosystem-scale iron fertilization experiment in the equatorial Pacific Ocean: Nature, v. 383, p. 495–501.
Coetzee, L.L., ms, 2001, Genetic stratigraphy of the Paleoproterozoic Pretoria Group in the western Transvaal: M.S. thesis, Rand Afrikaans University, Johannesburg, 195 p.
Corfu, F., and Andrews, A. J., 1986, A U-Pb age for mineralized Nipissing diabase, Gowganda, Ontario: Canadian Journal of Earth Sciences, v. 23, p. 107–109.
Cornell, D. H., Armstrong, R. A., and Walraven, F., 1998, Geochronology of the Proterozoic Hartley Basalt Formation, South Africa: constraints on the Kheis tectogenesis and the Kaapvaal Craton's earliest Wilson cycle: Journal of African Earth Sciences, v. 26, p. 5–27.
Cornell, D. H., Schütte, S. S., and Englinton, B. L., 1996, The Ongeluk basaltic andesite formation in Griqualand West, South Africa: submarine alteration in a 2222 Ma Proterozoic sea: Precambrian Research, v. 79, p. 101–123.
Corsetti, F. A., and Kaufman, A. J., 1999, Tossing Neoproterozoic snowballs between Death Valley, USA and Namibia: Geological Society of America, Annual Meeting, Abstracts with Programs, v. 31, no. 7, p. A-486.
Derry, L. A., Kaufman, A. J., and Jacobsen, S. B., 1992, Sedimentary cycling and environmental change in the Late Proterozoic: evidence from stable and radiogenic isotopes: Geochimica et Cosmochimica Acta, v. 56, p. 1317–1329.
Des Marais, D. J., 1997, Isotopic evolution of the biogeochemical carbon cycle during the Proterozoic Eon: Organic Geochemistry, v. 27, no. 5–6, p. 185–193.
Des Marais, D. J., Strauss, H., Summons, R. E., and Hayes, J. M., 1992, Carbon isotope evidence for the stepwise oxidation of the Proterozoic environment: Nature, v. 359, p. 605–609.
Dorland, H. C., ms, 1999, Paleoproterozoic laterites, red beds and ironstones of the Pretoria Group with reference to the history of atmospheric oxygen: M.S. thesis, Rand Afrikaans University, Johannesburg, 147 p.
Eriksson, P. G., and Reczko, B. F. F., 1998, Contourites associated with pelagic mudrocks and distal delta-fed turbidites in the Lower Proterozoic Timeball Hill Formation epeiric basin (Transvaal Supergroup), South Africa: Sedimentary Geology, v. 120, p. 319–335.
Evans, D. A., Beukes, N. J., and Kirschvink, J. L., 1997, Low-latitude glaciation in the Paleoproterozoic era: Nature, v. 386, p. 262–266.
Fairchild, I. J., Marshall, J. D., and Bertrand-Sarfati, J., 1990, Stratigraphic shifts in carbon isotopes from Proterozoic stromatolitic carbonates (Mauritania): influence of primary mineralogy and diagenesis: American Journal of Science, v. 290-A, p. 46–79.
Falkowski, P. G., Barber, R. T., and Smetacek, V., 1998, Biogeochemical controls and feedbacks on ocean primary productivity: Science, v. 281, p. 200–206.
Farquhar, J., Bao, H., and Thiemens, M., 2000, Atmospheric influence of Earth's earliest sulfur cycle: Science, v. 289, p. 756–758.
Freeman, K. H., and Hayes, J. M., 1992, Fractionation of carbon isotopes by phytoplankton and estimates of ancient CO_2 levels: Global Biogeochemical Cycles, v. 6, p. 185–198.
Gorokhov, I. M., Semikhatov, M. A., Baskakov, A. V., Kutyavin, E. P., Mel'nikov, N. N., Sochava, A. V., and Turchenko, T. L., 1995, Sr isotopic composition in Riphean, Vendian, and Lower Cambrian carbonates from Siberia: Stratigraphy and Geological Correlation, v. 3, p. 1–28.

Grotzinger, J. P., 1994, Trends in Precambrian carbonate sediments and their implication for understanding evolution, *in* Bengtson, S., editor, Early Life on Earth, Nobel Symposium no. 84: New York, Columbia University Press, p. 245–258.
Gutzmer, J., and Beukes, N. J., 1996, Karst-hosted fresh-water Paleoproterozoic Manganese deposits, Postmasburg, South Africa: Economic Geology, v. 91, p. 1435–1454.
Hattori, K., Krouse, H. R., and Campbell, F. A., 1983, The start of sulfur oxidation in continental environments: about 2.2×10^9 years ago: Science, v. 221, p. 549–551.
Hayes, J. M., 1983, Geochemical evidence earing on the origin of the aerobiosis; a speculative hypothesis, *in* Schopf, J. W., editor, Earth's Earliest Biosphere: Its origin and evolution: Princeton, New Jersey, Princeton University Press, p. 291–301.
Hayes, J. M., Kaplan, I. R., and Wedeking, K. W., 1983, Precambrian organic geochemistry, preservation of the record, *in* Schopf, J. W., editor, Earth's Earliest Biosphere: Its origin and evolution: Princeton, New Jersey, Princeton University Press, p. 93–134.
Hayes, J. M., Strauss, H., and Kaufman, A. J., 1999, The abundance of ^{13}C in marine organic matter and isotopic fractionation in the global biogeochemical cycle of carbon during the past 800 Ma: Chemical Geology, v. 161, p. 103–125.
Heaman, L. M., 1997, Global mafic magmatism at 2.45 Ga: Remnants of an ancient large igneous province?: Geology, v. 25, p. 299–302.
Hegenberger, W., 1993, Stratigraphy and sedimentology of the late Precambrian Witvlei and Nama groups, east of Windhoek: Geological Survey of Namibia, Memoir 17, 82 p.
Hoffman, P. F., 1975, Shoaling-upward shale-to-dolomite cycles in the Rocknest Formation (lower Proterozoic), Northwest Territories, Canada, *in* Ginsburg, R. N., editor, Tidal deposits: New York, Springer-Verlag, p. 257–265.
Hoffman, P. F., Kaufman, A. J., Halverson, G. P., 1998, Comings and goings of global glaciations on a Neoproterozoic tropical platform in Namibia: GSA Today, v. 8, no. 5, p. 1–9.
Hoffman, P. F., Kaufman, A. J., Halverson, G. P., and Schrag, D. P., 1998, A Neoproterozoic Snowball Earth: Science, v. 281, p. 1342–1346.
Hoffman, P. F., and Schrag, D. P., 2000, Snowball Earth: Scientific American, no. 1, p. 68–75.
Holland, H. D., 1994, Early Proterozoic atmospheric change, *in* Bengston, S. editor, Early Proterozoic life on Earth, Nobel Symposium no. 84: New York, Columbia University Press, p. 237–241.
Isley, A. E., 1995, Hydrothermal plumes and the delivery of iron to banded iron formation: The Journal of Geology, v. 103, p. 169–185.
Iyer, S. S., Babinski, M., Krouse, H. R., and Chemale, F. Jr., 1995, Highly ^{13}C-enriched carbonate and organic matter in the Neoproterozoic sediments of the Bambuí Group, Brazil: Precambrian Research, v. 73, p. 271–282.
Jacobsen, S. B., and Kaufman, A. J., 1999, The Sr, C and O isotopic evolution of Neoproterozoic sea water: Chemical Geology, v. 161, p. 37–57.
Jasper, J. J., and Hayes, J. M., 1990, A carbon-isotopic record of CO_2 levels during the Late Quaternary: Nature, v. 347, p. 462–464.
Kah, L. C., and Knoll, A. H., 1996, Microbenthic distribution of Proterozoic tidal flats: envirnomental and taphonomic considerations: Geology, v. 24, p. 79–82.
Kah, L. C., Sherman, A. G., Narbonne, G. M., Knoll, A. H., and Kaufman, A. J., 1999, $\delta^{13}C$ stratigraphy of the Proterozoic Bylot Supergroup, Baffin Island, Canada: implications for regional lithostratigrpahic correlations: Canadian Journal of Earth Sciences, v. 36, p. 313–332.
Karhu, J. A., 1993, Paleoproterozoic evolution of the carbon isotope ratios of sedimentary carbonates in the Fennoscandian Shield: Geological Survey of Finland Bulletin 371, 87 p.
Karhu, J. A. and Holland, H. D., 1996, Carbon isotopes and the rise of atmospheric oxygen: Geology, v. 24, no. 10, p. 867–870.
Kasting, J. F., 1987, Theoretical constraints on oxygen and carbon dioxide concentrations in the Precambrian atmosphere: Precambrian Research, v. 34, p. 205–229.
Kaufman, A. J., 1997, An ice age in the tropics: Nature, v. 386, p. 227–228.
Kaufman, A. J., Hoffman, P. F., and Halverson, G. P., 1997, Comings and goings of Neoproterozoic ice ages in Namibia: Geological Society of America, Annual Meeting, Abstracts with Programs, v. 29, no. 7, p. A-196.
Kaufman, A. J., Jacobsen, S. B., and Knoll, A. H., 1993, The Vendian record of Sr and C isotopic variations in seawater: Implications for tectonics and paleoclimate: Earth and Planetary Science Letters, v. 120, p. 409–430.
Kaufman, A. J., and Knoll, A. H., 1995, Neoproterozoic variations in the C-isotopic composition of seawater: stratigraphic and biogeochemical implications: Precambrian Research, v. 73, p. 27–49.
Kaufman, A. J., Knoll, A. H., and Awramik, S. M., 1992, Biostratigraphic and chemostratigraphic correlation of Neoproterozoic sedimentary successions: Upper Tindir Group, northwestern Canada, as a test case: Geology, v. 20, p. 181–185.
Kaufman, A. J., Knoll, A. H., and Narbonne, G. M., 1997, Isotopes, ice ages, and terminal Proterozoic earth history: National Academy of Science, Proceedings, v. 94, p. 6600–6605.
Kennedy, M. J., Runnegar, B., Prave, A. R., Hoffmann, K.-H., Arthur, M. A., 1998, Two or four Neoproterozoic glaciations?: Geology, v. 26, p. 1059–1063.
Kirschvink, J. L., 1992, Late Proterozoic low-latitude global glaciation: the snowball Earth, *in* J. W. Schopf and C. Klein, editors, The Proterozoic biosphere: a multidisciplinary study: Cambridge, United Kingdom, Cambridge University Press, p. 51–52.
Kirschvink, J. L., Gaidos, E. J., Bertani, L. E., Beukes, N. J., Gutzmer, J., Maepa, L. N., and Steinberger, R. E., 2000, The Paleoproterozoic Snowball Earth: extreme climatic and geochemical global change and its biological consequences: National Academy of Science, Proceedings v. 97, p. 1400–1405.

Knoll, A. H., Kaufman, A. J., and Semikhatov, M. A., 1995, The carbon isotopic composition of Proterozoic carbonates: Riphean successions from northwestern Siberia (Anabar Massif, Turukhansk Uplift): American Journal of Science, v. 295, p. 823–850.

Krogh, T. E., Davis, D. W., and Corfu, F., 1984, Precise U-Pb zircon and baddeleyite ages for the Sudbury area, *in* Pye, E. G., Naldrett, A. J., and Giblin, P. E., editors, The Geology and ore deposits of the Sudbury structure: Ontario Geological Survey, Special Volume 1, p. 431–446.

Kump, L. R., Arthur, M. A., Patzkowsky, M. E., Gibbs, M. T., Pinkus, D. S., and Sheehan, P. M., 1999, A weathering hypothesis for glaciation at high atmospheric pCO_2 during the Late Ordovician: Palaeogeography, Palaeoclimatology, Palaeoecology, v. 152, p. 173–187.

Li, R., Chen, J., Zhang, S., Lei, J., Shen, Y., and Chen, X., 1999, Spatial and temporal variations in carbon and sulfur isotopic compositions of Sinian sedimentary rocks in the Yangtze platform, South China: Precambrian Research, v. 97, pp. 59–75.

Marmo, J. S., 1992, The Lower Proterozoic Hokkalampi Paleosol in North Karelia, Eastern Finland, *in* Schidlowski, M., Golubic, M., Kimberley, M. M., McKirdy, D. M., and Trudinger, P. A., editors, Early Organic Evolution: Implications for Mineral and Energy Resources: Berlin, Germany, Springer-Verlag, p. 41–66.

Martin, D. McB., Clendenin, C. W., Krapez, B., and McNaughton, N. J., 1998, Tectonic and geochronological constraints on late Archaean and Palaeoproterozoic stratigraphic correlation within and between the Kaapvaal and Pilbara Cratons: Journal of the Geological Society, London, v. 155, p. 311–322.

Martini, J. E. J., 1979, A copper-bearing bed in the Pretoria Group in Northeastern Transvaal, in Geokongress '77: Geological Society of South Africa Special Publication 6, p. 65–72.

Master, S., Verhagen, B. H., Bassot, J. P., Beukes, N. J., and Lemoine, S., 1993, Stable isotopic signatures of Paleoproterozoic carbonate rocks from Guinea, Senegal, South Africa and Zimbabwe: constraints on the timing of the ca. 2.0 Ga "Lomagundi" $\delta^{13}C$ excursion, Symposium: Early Proterozoic geochemical and structural constraints – metallogeny: Publication Occasionnelle 1993/23, p. 38–41.

McNaughton, N. J., and Pollard, P. J., 1993, Cassiterite: Potential for direct dating of mineral deposits and a precise age for the Bushveld Complex granites: comments and reply: Geology, v. 21, p. 285–286.

Melezhik, V. A., and Fallick, A. E., 1996, A widespread positive $\delta^{13}C_{carb}$ anomaly at around 2.33 - 2.06 Ga on the Fennoscandian Shield: a paradox?: Terra Nova, v. 8, p. 141–157.

Melezhik, V. A., Fallick, A. E., and Clark, T., 1997, Two billion year old isotopically heavy carbon: evidence from the Labrador Trough, Canada: Canadian Journal of Earth Sciences, v. 34, p. 271–285.

Melezhik, V. A., Fallick, A. E., Medvedev, P. V., and Makarikhin, V. V., 1999, Extreme $^{13}C_{carb}$ enrichment in ca. 2.0 Ga magnesite-stromatolite-dolomite- 'red beds' association in a global context: a case for the world-wide signal enhanced by a local environment: Earth-Science Reviews, v. 48, p. 71–120.

Mertanen, S., Halls, H. C., Vuollo, J. I., Pesonen, L. J., and Stepanov, V. S., 1999, Paleomagnetism of 2.44 Ga mafic dikes in Russian Karelia, eastern Fennoscandian Shield – implications for continental reconstructions: Precambrian Research, v. 98, p. 197–221.

Misi, A., and Veizer, J., 1998, Neoproterozoic carbonate sequences of the Una Group, Irece Basin, Brazil: chemostratigraphy, age and correlations: Precambrian Research, v. 89, p. 87–100.

Montañez, I. P., Banner, J. L., Osleger, D. A., Borg, L. E., Bosserman, P. J., 1995, Integrated Sr isotope variations and sea-level history of Middle to Upper Cambrian platform carbonates: Implications for the evolution of Cambrian seawater $^{87}Sr/^{86}Sr$: Geology, v. 24, p. 917–920.

Nelson, D. R., Trendall, A. F., and Altermann, W., 1999, Chronological correlations between the Pilbara and Kaapvaal cratons: Precambrian Research, v. 97, p. 165–189.

Ohmoto, H., 1997, When did the Earth's atmosphere become oxic?: The Geochemical News, no. 93, p. 12–13, 26–27.

Ojakangas, R. W., 1985, Evidence for Early Proterozoic glaciation: the dropstone unit - diamictite association: Geological Survey of Finland, Bulletin 331, p. 51–72.

Park, J. K., 1997, Paleomagnetic evidence for low-latitude glaciation during deposition of the Neoproterozoic Rapitan Group, Mackenzie Mountains, N.W.T., Canada: Canadian Journal of Earth Sciences, v. 34, p. 34–49.

Pedersen, T. F., and Calvert, S. E., 1990, Anoxia vs. productivity; what controls the formation of organic carbon rich sediments and sedimentary rocks: American Association of Petroleum Geologists Bulletin, v. 74, p. 454–466.

Popp, B. N., Laws, E. A., Bidigare, R. R., Dore, J. E., Hanson, K. L., and Wakeham, S. G., 1998, Effect of phytoplankton cell geometry on carbon isotope fractionation: Geochimica et Cosmochimica Acta, v. 62, p. 69–77.

Rainbird, R. H., and Donaldson, J. A., 1988, Nonglaciogenic deltaic deposits in the early Proterozoic Gowganda Formation, Cobalt Basin, Ontario: Canadian Journal of Earth Sciences, v. 25, p. 710–724.

Rainbird, R. H., Nesbitt, H. W., and Donaldson, J. A., 1990, Formation and diagenesis of sub-Huronian saprolith: comparison with a modern weathering profile: Journal of Geology, v. 98, p. 801–822.

Reczko, B. F. F., Eriksson, P. G., and Snyman, C. P., 1995, Some evidence for the base-metal potential of the Pretoria Group: stratigraphic targets, tectonic setting and REE patterns: Mineralum Deposita, v. 30, p. 162–167.

Riebesell, U., Wolf-Gladrow, D. A., and Smetacek, V., 1993, Carbon dioxide limitation of marine phytoplankton growth rates: Nature, v. 361, p. 249–251.

Rye, R., and Holland, H. D., 1998, Paleosols and the evolution of atmospheric oxygen: A critical review: American Journal of Science, v. 298, p. 621–672.

Schidlowski, M., Eichmann, R., and Junge, C., 1976, Carbon isotope geochemistry of the Precambrian Lomagundi carbonate province, Rhodesia: Geochimica et Cosmochimica Acta, v. 40, p. 449–455.

——— 1975, Precambrian sedimentary carbonates: Carbon and oxygen isotope geochemistry and implications for the terrestrial oxygen budget: Precambrian Research, v. 2, p. 1–69.

Schmidt, P. W., and Williams, G. E., 1999, Paleomagnetism of the Paleoproterozoic hematitic breccia and paleosol at Ville-Marie, Québec: further evidence for the low paleolatitude of Huronian glaciation: Earth and Planetary Science Letters, v. 172, p. 273–285.

Schmidt, P. W., Williams, G. E., and Embleton, B. J. J., 1991, Low palaeolatitude of Late Proterozoic glaciation: early timing of remanence in haematite of the Elatina Formation, South Australia: Earth and Planetary Science Letters, v. 105, p. 355–367.

Schreiber, U. M., and Eriksson, P. G., 1992, An Early Paleoproterozoic braid-delta system in the Pretoria Group, Transvaal Sequence, South Africa: Journal of African Earth Sciences, v. 15, no. 1, p. 111– 125.

Simonson, B. M., and Hassler, S. W., 1996, Was the deposition of large Precambrian iron formations linked to major marine transgressions?: The Journal of Geology, v. 104, p. 665–676.

Sohl, L. E., Christie-Blick, N., and Kent, D. V., 1999, Paleomagnetic polarity reversals in Marinoan (ca. 600 Ma) glacial deposits of Australia: Implications for the duration of low-latitude glaciation in Neoproterozoic time: Geological Society of America Bulletin, v. 111, p. 1120–1139.

Steyn, M. v. R., Gardyne, W. N., and Klop, A. A. C., 1986, The Gopane manganese deposits, Bophuthatswana, *in* Anhaeusser, G. R., and Maske, S., editors: Mineral deposits of Southern Africa, v. 2, p. 985–989.

Summons, R. E., Jahnke, L. L., Hope, J. M., and Logan, G. A., 1999, 2-Methylhopanoids as biomarkers for cyanobacterial oxygenic photosynthesis: Nature, v. 400, p. 554–557.

Sumner, D. Y., and Bowring, S. A., 1996, U-Pb geochronologic constraints on deposition of the Campbellrand Subgroup, Transvaal Supergroup, South Africa: Precambrian Research, v. 79, p. 25–35.

Sumner, D. Y., and Grotzinger, J. P., 1993, Numerical modelling of ooid size and the problem of Neoproterozoic giant ooids: Journal of Sedimentary Petrology, v. 63, p. 974–982.

Swart, Q. D., ms., 1999, Carbonate rocks of the Paleoproterozoic Pretoria and Postmasburg Groups, Transvaal Supergroup: M.S. thesis, Rand Afrikaans University, Johannesburg, South Africa, 126 p.

Swett, K., and Knoll, A. H., 1989, Marine pisolites from Upper Proterozoic carbonates of East Greenland and Spitsbergen: Sedimentology, v. 36, p. 75–93.

Tsikos, H., and Moore, J. M., 1997, Petrography and geochemistry of the Paleoproterozoic Hotazel Iron-Formation, Kalahari Manganese Field, South Africa: implications for Precambrian manganese metallogenesis: Economic Geology, v. 92, p. 87–97.

Tucker, M. E., 1986, Formerly aragonitic limestones associated with tillites in the Late Proterozoic of Death Valley, California: Journal of Sedimentary Petrology, v. 56, p. 818–830.

Urban, H., Stribrny, B., and Lippolt, H. J., 1992, Iron and manganese deposits of the Urucum District, mato Grosso do Sul, Brazil: Economic Geology, v. 87, p. 1375–1392.

Valley, J., 1986, Stable isotope geochemistry of metamophic rocks, *in* Valley, J. W., Taylor, H. P., and O'Neil, J. R., editors, Stable isotopes in high temperature geological processes: Mineralogical Society of America Reviews in Mineralogy, v. 26, p. 445–489.

Van Capellan, P., and Ingall, E. D., 1994, Benthic phosphorous regeneration, net primary production and ocean anoxia: A model for coupled marine biogeochemical cycles of carbon and phosphorous: Paleoceanography, v. 9, p. 677–692.

Veizer, J., 1983, Chemical diagenesis of carbonates: theory and application, *in* Arthur, M. A., Anderson, T. F., Kaplan, I. R., Veizer, J., and Land, L. S., editors, Stable isotopes in Sedimentary Geology: Society of Economic Paleontologists and Mineralogists, Short Course, 10: 3-1–3-100.

Veizer, J., Clayton, R. N., and Hinton, R. W., 1992, Geochemistry of Precambrian carbonates: IV. Early Paleoproterozoic (2.25 ± 0.25 Ga) seawater: Geochimica et Cosmochimica Acta, v. 56, p. 875–885.

Veizer, J., Plumb, K. A., Clayton, R. N., Hinton, R. W., and Grotzinger, J. P., 1992, Geochemistry of Precambrian carbonates: V. Late Paleoproterozoic seawater: Geochimica et Cosmochimica Acta, v. 56, p. 2487–2501.

Visser, J. N. J., 1971–1972, The Timeball Hill Formation at Pretoria - A prograding shore-line deposit: Annals of the Geological Survey, Pretoria (South Africa), v. 9, p. 115–118.

——— 1981, The Mid-Precambrian tillite in the Griqualand West and Transvaal Basins, South Africa, *in* Hambrey, M. J., and Harland, W. B., editors, Earth's pre-Pleistocene glacial record: New York, Cambridge University Press, p. 180–184.

Walraven, F., 1997, Geochronology of the Rooiberg Group, Transvaal Supergroup, South Africa: Economic Geology Research Unit, University of the Witwatersrand, Information Circular, v. 316, 21 p.

Walraven, F., Armstrong, R. A., and Kruger, F. J., 1990, A chronostratigraphic framework for the north-central Kaapvaal craton, the Bushveld Complex and the Vredefort structure: Tectonophysics, v. 171, p. 23–48.

Williams, G. E., and Schmidt, P. W., 1997, Paleomagnetism of the Paleoproterozoic Gowganda and Lorrain formations, Ontario: low paleolatitude for Huronian glaciation: Earth and Planetary Science Letters, v. 153, p. 157–169.

Williams, H., Hoffman, P. F., Lewry, J. F., Monger, J. W. H., and Rivers, T., 1991, Anatomy of North America: thematic geologic portrayals of the continent: Tectonophysics, v. 187, p. 117–134.

Wood, J., 1979, No. 18 Regional Geology of the Cobalt Embayment, District of Sudbury, Nipissing, and Timiskaming: Summary of Fieldwork, Ontario Geological Survey, Miscellaneous paper 90, p. 79–81.

Young, G. M., 1973, Tillites and aluminous quartzites as possible time markers for middle Precambrian (Aphebian) rocks of North America, *in* Young, G. M., editor, Huronian Stratigraphy and Sedimentation: Geological Association of Canada, Special Paper, 12, p. 97–127.

Young, G. M., 1988, Proterozoic plate tectonics, glaciation and iron-formations: Sedimentary Geology, v. 58, p. 127–144.